Sustained visual priming effects can emerge from attentional oscillation and temporal expectation

Muzhi Wang[1], Yan Huang[2], Huan Luo[1,3], Hang Zhang[1,3,4*]

1. School of Psychological and Cognitive Sciences and Beijing Key Laboratory of Behavior and Mental Health, Peking University, Beijing, China
2. Brain Cognition and Brain Disease Institute for Collaboration Research of SIAT at CAS and the McGovern Institute at MIT, Shenzhen Institutes of Advanced Technology, Chinese Academy of Sciences, Shenzhen, China
3. PKU-IDG/McGovern Institute for Brain Research, Peking University, Beijing, China
4. Peking-Tsinghua Center for Life Sciences, Beijing, China

*Corresponding author:

Hang Zhang, email: hang.zhang@pku.edu.cn

Short title: Oscillated temporal expectation model

Abstract

Priming refers to the influence that a previously encountered object exerts on future responses to similar objects. For many years, visual priming has been known as a facilitation and sometimes an inhibition effect that lasts for an extended period of time. It contrasts with the recent finding of an oscillated priming effect where facilitation and inhibition alternate over time periodically. Here we developed a computational model of visual priming that combines rhythmic sampling of the environment (attentional oscillation) with active preparation for future events (temporal expectation). Counterintuitively, it shows both the sustained and oscillated priming effects can emerge from an interaction between attentional oscillation and temporal expectation. The interaction also leads to novel predictions such as the change of visual priming effects with temporal expectation. Reanalysis of two published datasets and the results of one new experiment of visual priming tasks provide support for the model's relevance to human behavior.

Keywords: visual attention, visual priming, response time, behavioral oscillation, temporal expectation, temporal uncertainty

Introduction

Prior encounter with an object may speed up one's response to a similar object, a pervasive phenomenon in human cognition known as priming (Schacter and Buckner, 1998; Tulving and Schacter, 1990). The visual priming task has proved to be a powerful behavioral paradigm in probing the temporal dynamics of human attention (Eimer and Schlaghecken, 2003). In its simplest version (Figure 1A), participants judge the pointing direction of a target arrow preceded by a congruent or incongruent prime. The priming effects—response time (RT) for incongruent trials minus RT for congruent trials—may vary with the prime-to-target delay ("SOA"). Classic findings include sustained positive priming in unmasked priming tasks (Neumann and Klotz, 1994) and transient positive priming followed by sustained negative priming in masked priming tasks (Eimer, 1999; Eimer and Schlaghecken, 1998).

Recently, a theta-band (3–5 Hz) RT oscillation has been separated from these classic priming effects by spectral methods (Huang et al., 2015): RT fluctuates up and down as a function of SOA in cycles of approximately 300 msec, with the peaks of congruent trials accompanied by the valleys of incongruent trials and vice versa (Figure 1DH). Such ongoing oscillations are visually pronounced even on the individual level (Figure 4 of Huang et al., 2015). The finding of oscillated priming was a surprise but not entirely unexpected. On one hand, there are clues of oscillated priming in the literature—priming effects may first go up, then down, and up again when SOA goes from 0 to 300 msec (Lingnau and Vorberg, 2005) and similar patterns are observed in lateralized EEG signals related to motor preparation (Praamstra and Seiss, 2005). On the other hand, theta-band behavioral oscillations are widely observed in human perception (Benedetto and Morrone, 2017; Landau et al., 2015; Tomassini et al., 2015; Wutz et al., 2016; see

VanRullen, 2016 for a review), which may reflect a rhythmic perceptual sampling of the environment.

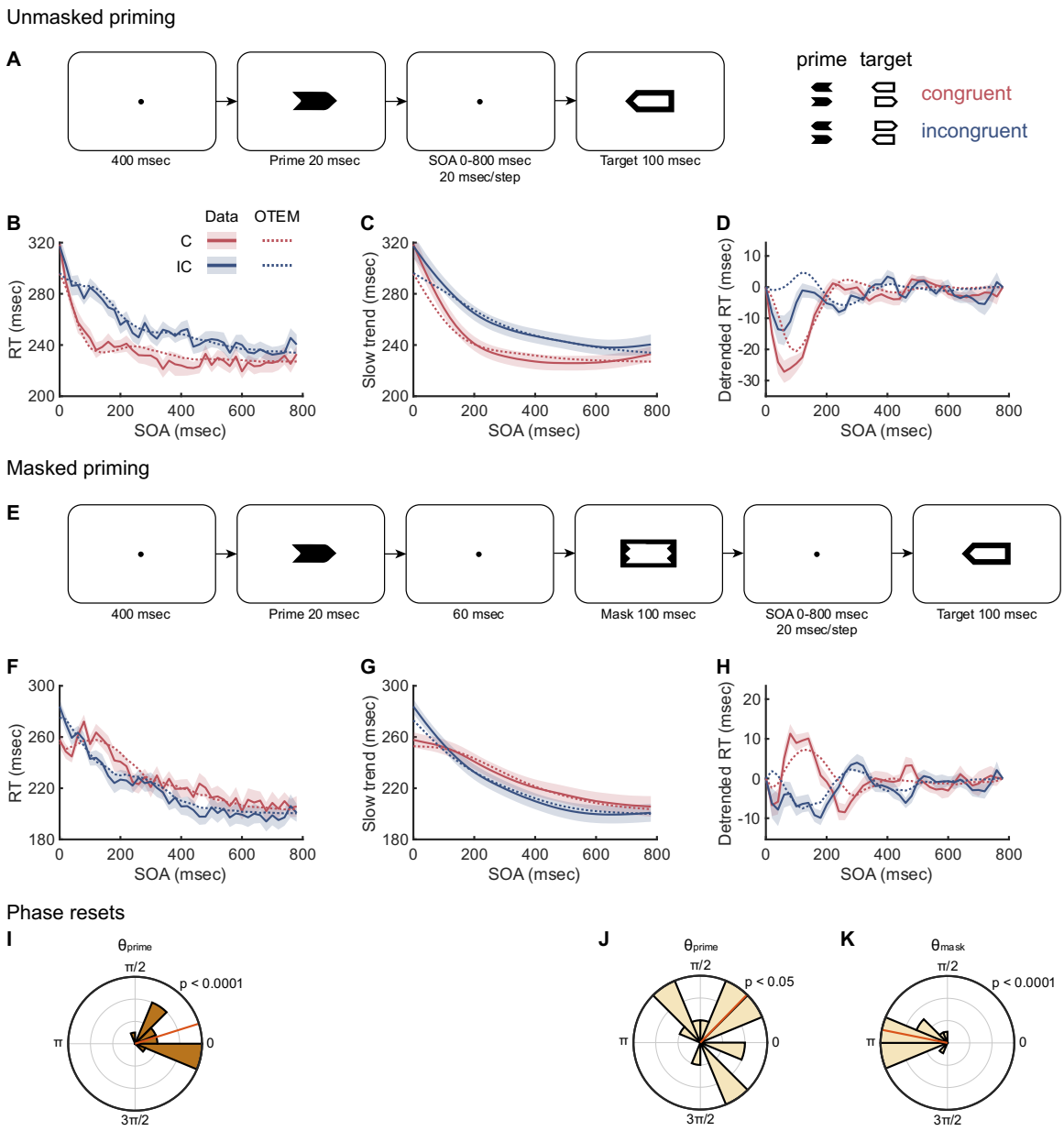

Figure 1. Oscillated Temporal Expectation Model (OTEM) reproduces the three priming effects in Huang et al. (2015). A, unmasked priming task. Participants reported the pointing direction of the target arrow by key press. When the prime and the target pointed to the same direction, they were congruent (*C*), otherwise incongruent (*IC*). The interval between the prime and the target was referred as SOA. **B,** mean RT as a function of SOA in the unmasked priming task, separately for the congruent (red) and incongruent (blue). Solid lines denote data. Dotted lines denote OTEM fits. Shadings denote SEM. Following

Huang et al. (2015), raw RTs of the unmasked priming task (**B**) were decomposed into slow trends (**C**) and detrended RTs (**D**), where positive priming (**C**) and oscillated priming (**D**) were observed. **E**, masked priming task. The same as unmasked priming task except that a mask followed the prime and the interval between the mask and the target was referred as SOA. **F**, mean RT as a function of SOA in the masked priming task, where positive priming followed by negative priming (slow trends, **G**) and oscillated priming (detrended RTs, **H**) were observed. **I**, Phase of attentional oscillation reset by the prime in the unmasked priming task. **J**, **K**, phases of attentional oscillation reset by the prime and the mask in the masked priming task. θ_{prime} and θ_{mask} were parameters of OTEM estimated from data. Rose plot shows the distribution of θ_{prime} or θ_{mask} across participants, which had significantly coherent values (Rayleigh tests, with *p* values marked on panels). The mean phase (red line) was close to 0 for θ_{prime} and to π for θ_{mask}. That is, attention is biased towards the congruent in the next half cycle following the prime and towards the incongruent in the next half cycle following the mask.

We performed additional analysis to confirm that the oscillated priming found in Huang et al. (2015) is not an artifact (Figure 1-figure supplement 2). Moreover, similar oscillatory effects in RT (Song et al., 2014) as well as in accuracy (Chen et al., 2017) have been recently reported in spatial cueing tasks, in addition to the classic sustained facilitation or inhibition effects at the cued location (Klein, 2000; Posner and Cohen, 1984).

What may explain the coexistence of the classic and oscillated cueing/priming effects, which seem to suggest two conflicting time schedules for attention orienting? Previous theories on spatial cueing (Klein, 2000; Nobre and Rohenkohl, 2014) or visual priming (Bowman et al., 2006; Eimer and Schlaghecken, 2003; Huber, 2014; Lleras and Enns, 2004; Sumner, 2007) have been devoted to the classic effects, which apparently cannot predict any ongoing oscillations. To explain the oscillatory RT effects, an attentional oscillation mechanism seems to be necessary. An additional factor that may have a major impact on RT but is largely neglected by previous cueing/priming theories is temporal expectation. Even though the cue/prime is non-informative about the identity

of the target, it signals the countdown to the target arrival. Temporal expectation has thus been assumed in the foreperiod task (Los et al., 2014; Los and Van Den Heuvel, 2001; Luce, 1986; Niemi and Näätänen, 1981; Nobre et al., 2007) to account for the decrease of RT with increasing SOA and is likely to explain a similar RT effect in cueing/priming (e.g. Figure 1BF).

Here we proposed a computational model that introduces attentional oscillation and temporal expectation into the visual priming task to predict the RT patterns. Its basic idea is close to “active sensing” (Lakatos et al., 2013, 2008) that the perceptual system actively predicts and prepares for potential future events (Nobre and van Ede, 2017; Summerfield and de Lange, 2014). Meanwhile, theta-band attentional oscillations provide fine-grained temporal windows of excitation and inhibition for the accumulation of preparedness (van Vugt et al., 2012). We call the model Oscillated Temporal Expectation Model (OTEM), whose key assumptions are illustrated in Figure 2 and unfolded in the Results. In brief, OTEM predicts not only the oscillated priming effect and the decrease of RT with increasing SOA, but also the classic priming effects. That is, sustained positive and negative priming effects can arise as emergent properties of the model, despite that no sustained excitation or inhibition mechanisms are assumed.

We tested OTEM quantitatively by first fitting it to the behavioral datasets of the unmasked and masked priming experiments in Huang et al. (2015) and found that it well reproduced all the priming effects as well as the overall RT patterns. Next, we performed a new experiment to test the functioning of temporal expectation, a key assumption that distinguishes OTEM from previous accounts of visual priming effects (Bowman et al., 2006; Boy and Sumner, 2010; Vorberg et al., 2003). As predicted, the visual priming effects were influenced not only by SOA but also by temporal expectation. Third, we tested two alternative models and found neither of them could reproduce all the priming

effects. Last, we showed that OTEM can be extended to predict error rates and atypical priming effects in the literature.

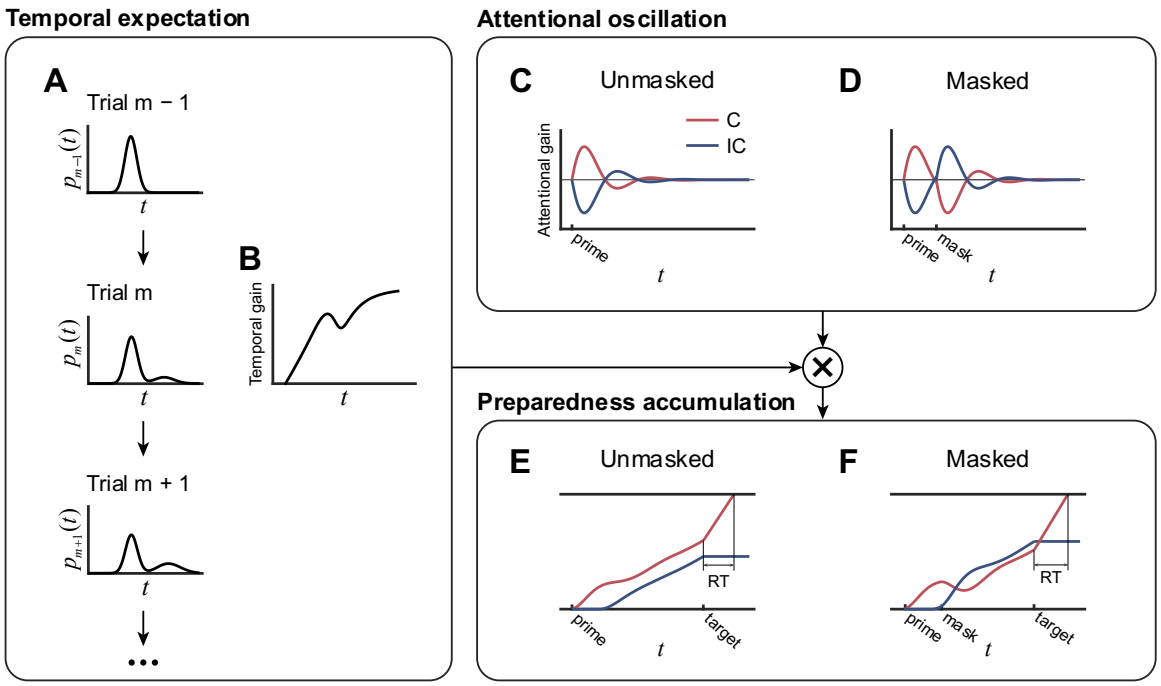

Figure 2. Illustration of the assumptions of OTEM. Temporal expectation: After each trial, the belief of SOA distribution ($p_m(t)$) is updated following the delta rule (**A**). Within a specific trial, the temporal gain (**B**) is computed based on $p_m(t)$ and updated from moment to moment until target onset. **Attentional oscillation**: The attentional gain for the congruent (*C*, in red) and incongruent (*IC*, in blue) oscillates over time, whose amplitude and phase are reset by the prime and the mask (**C**, **D**). **Preparedness accumulation**: Before target onset, two threads of preparedness accumulate over time separately for the congruent and incongruent, with the accumulating speed at each moment determined by the product of the corresponding attentional and temporal gains (**E**, **F**). After target onset, only the thread for the realized target continues to accumulate until it reaches the responding bound. The RT for a specific target is thus determined by the preparedness accumulated for the target up to its onset. Intuitively, the attentional oscillation in the unmasked priming task (**C**) gives the congruent thread a head start in the race (**E**), thus leading to sustained positive priming. In contrast, the mask in the masked priming task resets attentional oscillation (**D**) and reverses the ranking of the congruent and incongruent threads (**F**), thus leading to transient positive priming followed by sustained negative priming.

Results

Oscillated Temporal Expectation Model (OTEM)

The key assumptions of OTEM (Figure 2) is specified below (see Methods for details). For fluency of presentation, we only briefly describe their motivations here and leave a full treatment of the justification and implications of the assumptions to the Discussion.

Preparedness accumulation. We assume that responses are generated by an accumulation-to-bound process analogous to the racing models of perceptual decision-making (Luce, 1986). After the onset of the prime, two threads of preparation are separately accumulated for the two prospective targets—the congruent and incongruent—until the target arrives (Cisek, 2007; Cisek and Kalaska, 2010), after which only the preparedness for the realized target continues to accumulate. A response occurs when the responding bound is reached. The response time for a specific target is thus determined by the preparedness accumulated for the target up to its onset.

Temporal expectation. We assume that a belief of SOA distribution is learned from past trials following the delta rule (Rescorla and Wagner, 1972). On each trial, the brain uses this distribution as its (probabilistic) temporal expectation for the SOA of the incoming target and, as time elapses, keeps updating the expectation of remaining time until the target appears (de Lange et al., 2013; McGuire and Kable, 2013).

At any specific moment, the temporal expectation—a probability distribution over all future time points—decides how urgent the brain should prepare for prospective targets. To map the influence of the distribution to a single value, we introduce an economic concept: temporal discounting—the longer the expected delay of a reward, the lower the reward is valued in the brain (Frederick et al., 2002; Kable and Glimcher, 2007). In our case, it implies that the expected probability of target onset at a time point in the farther future has a smaller influence on the current preparing rate. Analogous to

171 the application of temporal discounting in the reinforcement learning literature (Sutton
172 and Barto, 1998), we assume that the preparing rate at a specific moment is proportional
173 to the *temporal gain* at the moment, defined as the expected sum of the temporally
174 discounted values of all future probabilities.

175 **Attentional oscillation.** There is increasing evidence that visual attention is a periodic
176 process that sequentially samples different alternatives in the theta frequency range
177 (Fiebelkorn et al., 2013; Kienitz et al., 2018; Landau et al., 2015; Landau and Fries, 2012;
178 Song et al., 2014; Tomassini et al., 2015; VanRullen, 2016). Following these empirical
179 findings, we assume that the focus of attention switches gradually between the two
180 prospective targets in theta-band oscillations, leading to anti-phased attentional gains for
181 the congruent and incongruent. The phase of the attentional oscillation is reset by the
182 prime and the mask, while its amplitude decreases exponentially with time, as suggested
183 by stimulus-induced resets of theta-band neuronal oscillations (Buzsáki, 2006; Makeig et
184 al., 2002; McCartney et al., 2004; Rizzuto et al., 2003; Tesche and Karhu, 2000) and
185 behavioral oscillations (Fiebelkorn et al., 2013; Landau and Fries, 2012; Song et al.,
186 2014). We assume that the preparing rate for the congruent or incongruent target is
187 scaled by its attentional gain as well as by the temporal gain.

188

189 OTEM reproduces both the classic and oscillated priming effects

190 The datasets of Huang et al. (2015) include one unmasked and one masked priming
191 experiments (Figure 1), where RTs for the congruent and incongruent varied as
192 functions of SOA. Fifty different SOAs were sampled for each experiment, in a 20-msec
193 step from 0 to 980 msec. Decomposing each raw RT curve into a slow trend and a
194 detrended curve, Huang et al. (2015) identified the classic and oscillated priming effects
195 respectively in the two components.

Given that the oscillated priming effect was the motive of our work, we performed additional analyses on these datasets to confirm that the oscillation was not an artifact from spectral analysis. It was noted that the specific moving-window detrending procedure used by Huang et al. (2015), with its edge artifact, might cause illusory theta-band oscillations in the detrended curve when it was applied to a simulated exponentially-decreasing RT curve without any oscillations. Simulations (Figure 1-figure supplement 2AB) show that the illusory theta-band oscillations would be eliminated if an exponential curve fitting were used for detrending. In contrast (Figure 1-figure supplement 2CD), the oscillated priming effect was still present when we applied the same exponential detrending procedure to the datasets of Huang et al. (2015). We further confirmed that there was an ongoing oscillation instead of just one beat in the detrended RTs: The theta-band power was still statistically significant even when the first 200 msec of SOAs were excluded (Figure 1-figure supplement 3).

We fit OTEM to the RTs of individual trials for correct responses for each participant using maximum likelihood estimates (see Figure 2-figure supplement 3 for the estimated parameters) and plot the model fits against data (Figure 1BF, dotted vs. solid curves). The OTEM fits captured the following patterns of the observed RT curves. First, the slow trends for both the congruent and incongruent trials decreased monotonically with SOA at a decreasing speed. Second, in the slow trends of the unmasked priming task (Figure 1C), positive priming (i.e. incongruent RTs above congruent RTs) persisted throughout all SOAs, with the difference between the incongruent and congruent RTs first increasing then decreasing. Third, in the slow trends of the masked priming task (Figure 1G), positive priming occurred for short SOAs (< 100 msec) and changed into negative priming (i.e. congruent RTs above incongruent RTs) for longer SOAs. Fourth, the detrended RT curves (Figure 1DH) oscillated at frequencies of 3–5 Hz and were anti-phased for the congruent and incongruent (see the

Figures 2 and 3 of Huang et al. (2015) for the observed frequency spectra and phase differences, and see Figure 1-figure supplement 1 for OTEM fits).

In other words, OTEM reproduces both the classic and oscillated priming effects. Given that theta-band attentional oscillations are assumed in OTEM, it is probably not surprising the model can predict the observed oscillated priming. However, the classic positive and negative priming are emergent properties of the model, since no persistent attentional biases towards the congruent or incongruent have been assumed. That is, these classic priming effects arise also from the attentional oscillations. According to the phase parameters estimated from data (Figure 1IJK), both the prime and the mask induced phase resets that were coherent across participants (Rayleigh test: unmasked prime, $r = 0.82$, $z = 10.87$, $p < 0.0001$; masked prime, $r = 0.41$, $z = 2.98$, $p = 0.049$; masked mask, r = 0.89, $z = 14.18$, $p < 0.0001$). On average, the prime reset the phases of the attentional gains for the congruent and incongruent oppositely to approximately 0 and π (in sine), so that the preparedness of the congruent would accumulate faster than the incongruent in the first half cycle. Conversely, the mask reset the congruent and incongruent phases to approximately π and 0, giving the incongruent an advantage in the subsequent half cycle.

Here is an intuition how the classic priming effects emerge from OTEM (see Figure 2 for illustrations): After the attentional oscillations are reset by the prime, the specific phase difference allows the attentional gain of the congruent to climb to the peak earlier than that of the incongruent, giving the congruent a lead in preparedness. For unmasked priming tasks, the congruent keeps the lead throughout the race despite that the congruent and incongruent receive alternating advantages in attentional gains, and thus positive priming is observed. For masked priming tasks, a second reset of the attentional oscillations by the mask reverses the lead, resulting in early positive priming and late negative priming.

The emergence of the classic priming effects from OTEM is insensitive to the choice of most parameters in OTEM. Except for the phase reset parameters, changing the parameters of OTEM would only alter the overall RT and the magnitudes of the priming effects but hardly the qualitative finding of the priming effects (Figure 2-figure supplement 1).

OTEM predicts the effects of temporal expectation

OTEM predicts that the RT of a trial should depend not only on its SOA (i.e. the actual moment of target onset), but also on the temporal expectation that is shaped by past trials. We tested this prediction in a new masked priming experiment, which consisted of four experimental conditions that used the same set of SOAs but differed in local temporal contexts. In the 40-SOA condition, 40 different SOAs (0 to 780 msec in a 20-msec step) were repeated in a random order, as in Huang et al. (2015). In the 20-SOA condition, the same 40 SOAs were divided into two blocks—the first 20 SOAs and last 20 SOAs, so that the SOA was expected to be within 0–380 msec for the former and within 400–780 msec for the latter. Similarly, the 10-SOA condition had 4 blocks of 10 SOAs and the 4-SOA condition had 10 blocks of 4 SOAs. In all the conditions, each SOA was repeated for 24 times (12 congruent + 12 incongruent) and the order of the blocks was randomized for each participant. In the same procedure applied to the datasets of Huang et al. (2015), we fit OTEM to the RTs of individual trials for each participant in each condition (see Figure 2-figure supplement 3 for the estimated parameters) and plot model fits against data (Figure 3A).

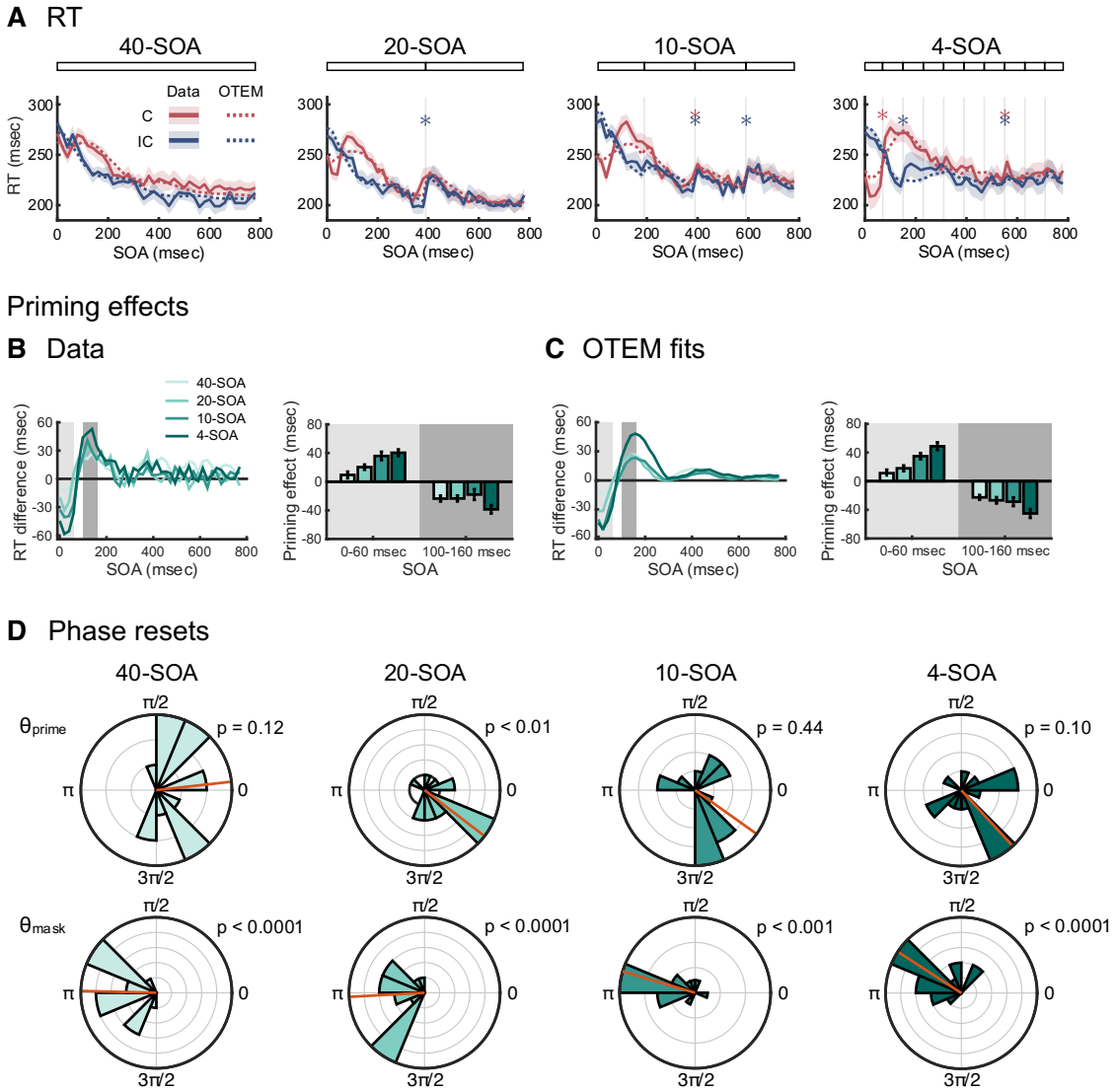

Figure 3. OTEM predicts the effects of temporal expectation in the new experiment. A, mean RT as a function of SOA, separately for the congruent (red) and incongruent (blue). Solid lines denote data. Dotted lines denote OTEM fits. Shadings denote SEM. Each panel is for one temporal context condition, with the experimental manipulation schematized above the panel (see text). Asterisks indicate statistically significant "jumps" at block borders ($p < 0.05$). **B**, observed priming effects and **C**, OTEM predicted priming effects as functions of SOA. Priming effects were computed as the difference in RT between the congruent and incongruent. Around the peaks of positive priming (light gray shading) and negative priming (dark gray shading), the magnitudes of mean priming effects (bar graphs) increased over the four conditions. **D**, phases of attentional oscillation reset by the prime

and the mask. Conventions follow Figure **1I**–**K**. The phases estimated in all four conditions were similar and resembled those of Huang et al. (2015) (see Figure **1I**–**K**).

We found distinctive RT patterns in the four conditions. The 40-SOA condition replicated the results of the masked priming experiment of Huang et al. (2015), including both the classic and oscillated priming effects (Figure 3-figure supplements 1 and 2), which would serve as a baseline. A hallmark of the other three conditions was a “jump” in RT at the border of two adjacent blocks, for example, the dramatic increase of RT from SOA=380 msec to SOA=400 msec in the 20-SOA condition. Out of the 26 block borders (separately for the congruent and incongruent) of the 20-SOA, 10-SOA, and 4-SOA conditions, 8 had significant RT increases (one-tailed *t*-tests, *p*s < 0.05). To assess the base rate of false positive increasing RTs, we performed *t*-tests for the same SOA pairs in the 40-SOA condition and had only one significant RT increase out of the 22 comparisons. The proportion of jumps at the block borders was significantly above the base rate (8/26 vs. 1/22, Fisher’s exact test, $p = 0.028$).

The OTEM fits agreed well with the observed RT patterns (Figure 3A). In particular, OTEM could predict the dramatic increase of RT at the borders of SOA blocks, although it makes no special assumptions about SOA blocks. According to OTEM, the closer the time approaches the last SOA of the block, the sooner the target is expected to arrive, the faster the accumulation of preparedness. Thus, the last SOA of a block could have a faster RT than the first SOA of its next block, despite the general decreasing trend of RT with SOA due to preparedness accumulation.

The magnitudes of priming effects differed across the four conditions (Figure 3B). Around the peak of positive priming (SOA = 0–60 msec), the mean priming effect (RT difference between the incongruent and congruent) went larger and larger from 40-SOA, 20-SOA, 10-SOA to 4-SOA (one-way ANOVA, $F(3,60) = 13.02$, $p < 0.001$). The mean

peaked negative priming effect (SOA = 100–160 msec) exhibited a similar pattern ($F(3,60) = 3.81$, $p = 0.014$). Both patterns were captured by OTEM fits (Figure 3C).

When the raw RT curve was decomposed into a slow trend and a detrended curve as in Huang et al. (2015), we observed similar theta-band oscillations in the detrended curves of all conditions (Figure 3-figure supplement 2). The estimated phase parameters in OTEM (Figure 3D) were indistinguishable across the four conditions (Watson-Williams test, $F(3,60) = 1.11$, $p = 0.35$ for prime phase; $F(3,60) = 2.08$, $p = 0.11$ for mask phase) and resembled those of the masked priming experiment in Huang et al. (2015). That is, the attentional oscillations were little influenced by the temporal context of the experiment.

As we mentioned earlier, OTEM correctly predicts that the different temporal expectations associated with different contextual blocks may lead to RT “jumps” at the block borders (Figure 3A). These quasi-periodic RT jumps should lead to perturbations at 2.5, 5, and 12.5 Hz in the detrended RT time series respectively for the 20-, 10-, and 4-SOA conditions, selectively enhancing or reducing specific frequency components. Some of the spectral perturbations predicted by OTEM fits were indeed observed in the data, most evident in the following two phenomena (Figure 3-figure supplement 2). First, there was a second or extended peak for the incongruent around theta-band in the 20- and 10-SOA conditions, respectively echoing the 2.5 and 5 Hz RT jumps. Second and counterintuitively, for the 20-SOA condition, OTEM predicted that the congruent-incongruent phase difference estimated from the detrended RTs should be close to 0 rather than to π, despite attentional oscillations were assumed to be anti-phased. This phase change was due to the vicinity of the frequency of perturbation (2.5 Hz) to the frequency of attentional oscillation (3.3 Hz). Consistent with the OTEM fits, the observed congruent-incongruent phase difference in the 20-SOA condition was close to 0, with the coherence across participants reaching marginal significance.

In addition, OTEM predicts that sequential effects would arise from the trial-by-trial updating of temporal expectation. When the preceding trials have longer SOAs, the temporal expectation for the current SOA would be longer, thus the preparing speed would be lower, resulting in a longer RT. We tested this prediction by regressing the current RT over the SOAs of the last three trials, with the RTs of the last three trials and the current SOA serving as nuisance covariates. As predicted, the coefficients for the last and sometimes up to the third last SOA were significantly greater than zero (Figure 4A), with the patterns of the data closely following those of the model fits (Figure 4B).

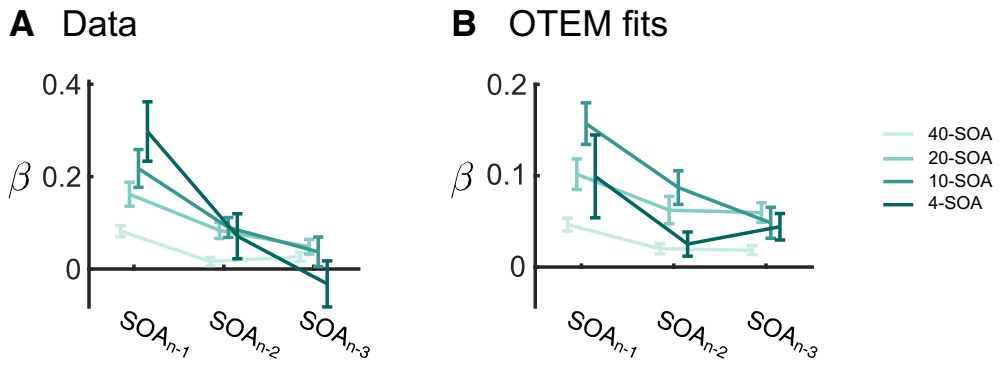

Figure 4. Sequential effects of SOAs. OTEM predicts that when the preceding trials have longer SOAs, the temporal expectation for the current SOA would be longer, thus the preparing speed would be lower, resulting in a longer RT. To quantify this possible sequential effect, we regressed the current RT over the SOAs of the last three trials, with the RTs of the last three trials and the current SOA serving as nuisance covariates. The regression coefficients (β) from OTEM fits (**B**) closely resembled the patterns of the data (**A**).

OTEM outperforms alternative models

We considered two alternative computational models that can produce visual priming effects. Among them, the “constant accumulation model” was based on the accumulator model of Vorberg et al. (2003). The original model, applying only to unmasked priming

356 tasks to explain positive priming, assumes that the prime triggers a constant-speed
357 accumulation of a decision variable towards the congruent. In the constant accumulation
358 model, we extended the model to masked priming tasks with the additional assumption
359 that the mask would change the direction of the constant accumulation towards the
360 incongruent, so that it can produce negative as well as positive priming effects.

361 A second alternative model was motivated by a widely-accepted idea in the
362 foreperiod task (Luce, 1986; Niemi and Näätänen, 1981; Nobre et al., 2007) that RT for
363 a delayed target depends on the urgency of response at target onset: The higher the
364 urgency, the shorter the RT. In particular, urgency is defined by hazard rate, that is, the
365 conditional probability the target is expected to occur at the next moment, given that it
366 has not occurred yet. To account for oscillated priming, attentional oscillation is assumed
367 as in OTEM. We call the model “oscillated urgency model”, whose assumptions are
368 otherwise the same as OTEM except for how temporal expectation influences RT: The
369 preparedness for the congruent or incongruent is proportional to the instantaneous
370 hazard rate instead of being accumulated over time (see Methods).

371 We fit the constant accumulation model and oscillated urgency model to the RT
372 data of Huang et al. (2015) and our new experiment using maximum likelihood estimates,
373 in the same procedure as we fit OTEM. The Akaike information criterion corrected for
374 small samples (Akaike, 1974; Hurvich and Tsai, 1989) was used as the metric of
375 goodness-of-fit and the protected exceedance probability (Rigoux et al., 2014; Stephan
376 et al., 2009)—the probability a specific model outperforms all the other models—was
377 calculated as the group-level measure for model comparison. For all the datasets,
378 OTEM outperformed the other two models in AICc and had protected exceedance
379 probabilities approaching 100% (Figure 3-figure supplement 3A).

380 The deviation of the constant accumulation model from data was obvious (Figure
381 3-figure supplement 3B): By definition, it could only predict two opposing RT trends for

382 the congruent and the incongruent—if one decreases with SOA, the other must increase
383 with SOA, a unique finding of Vorberg et al.'s (2003). In the case both the congruent and
384 incongruent RTs decrease with SOA, as in our datasets and most previous visual
385 priming studies (Eimer and Schlaghecken, 2003; Lleras and Enns, 2004; Sumner, 2007),
386 the constant accumulation model would simply fail. The problem with the oscillated
387 urgency model was its inability to produce an enduring positive or negative priming effect
388 (Figure 3-figure supplement 3C), though its assumptions of attentional oscillation and
389 temporal expectation are similar to those of OTEM. It is because the emergence of
390 positive and negative priming in OTEM relies on the accumulation of preparedness over
391 time as well as on attentional oscillation and temporal expectation. Without the
392 accumulation, the congruent and incongruent RTs would merely follow the fluctuation of
393 attentional oscillations.
394

395 **Extended OTEM explains error rates and atypical priming effects**

396 The OTEM introduced above only applies to correct responses, which make up
397 approximately 95% of the trials of most visual priming experiments including ours (Eimer,
398 1999; Eimer and Schlaghecken, 1998; Huang et al., 2015; Schlaghecken and Eimer,
399 2002; Verleger et al., 2004). The error rates, though small, could be patterned (Figure 3-
400 figure supplement 4A): In the 4-SOA condition, for example, the error rate of the
401 incongruent was higher than that of the congruent around the peak of positive priming
402 (0–60 msec), while it was the reverse around the peak of negative priming (100–160
403 msec). This cannot be explained by speed-accuracy trade-off, since the accuracy for fast
404 responses was even higher than that of slow responses. Such patterns—positive
405 priming is accompanied by a higher error rate for the incongruent and negative priming

by a higher error rate for the congruent—were also observed in previous studies using visual priming tasks (Eimer, 1999; Eimer and Schlaghecken, 1998; Vorberg et al., 2003).

To model error responses, we extended OTEM to include an additional decision process after target onset, where the congruent and incongruent accumulators race against and inhibit each other (see Methods). Consistent with the observed patterns, the extended OTEM predicts a higher error rate for the incongruent than the congruent at positive priming and the reverse pattern at negative priming (Figure 3-figure supplement 4B). The RTs and error rates are not cause and effect, but the effects of a common cause: When one accumulator has achieved a higher preparedness than the other at target onset, the subsequent decision process would be biased towards the leading accumulator. In an unmasked priming task, Vorberg et al. (2003) found that the congruent RT decreased with SOA but the incongruent RT increased with SOA, which deviated from the typical finding that both the congruent and incongruent RTs decrease with SOA (e.g. Figure 1B). They also found that error rate increased with SOA. We noticed, however, the SOAs they used were unusually short (no longer than 108 msec), so did all the following studies that had found similar RT patterns (Mattler and Palmer, 2012; Sack et al., 2009). Such short SOAs would be within the first half cycle of the attentional oscillation of OTEM (approximately 300 msec per cycle), where the attentional gain for the incongruent is still low. That is, the increase of RT with SOA for the incongruent and the decrease of RT with SOA for the congruent they observed can be part of oscillated priming. Using the same SOAs as in Vorberg et al. (2003), the extended OTEM can reproduce their RT and error rate patterns (Figure 3-figure supplement 4C).

Discussion

We developed OTEM as a computational model that combines attentional oscillation and temporal expectation to explain visual priming effects in RT and tested it in three human behavioral experiments. OTEM accurately reproduces all three kinds of priming effects—positive priming, negative priming, and oscillated priming, while the alternative models fail to do so. It correctly predicts temporal expectation would influence visual priming effects. It explains not only the averaged priming effects, but also trial-by-trial variations in RT. Most surprisingly, OTEM shows that the classic, sustained positive and negative priming effects can be emergent properties of attentional oscillation and temporal expectation, a prediction that qualitatively holds for a wide range of parameter values (Figure 2-figure supplement 1).

Relation to previous theories of visual priming effects

What causes the visual priming effects? In the past years, theories with incremental assumptions about a perceptual or motor bias have been proposed to explain the increasingly richer phenomena. Among the three priming effects, positive priming was first discovered, at which time the bias was assumed to be triggered by the prime to favor the congruent (Damian, 2001; Eimer, 1999; Eimer and Schlaghecken, 1998; Neumann and Klotz, 1994; Vorberg et al., 2003). When negative priming was later found in masked priming tasks, self-inhibition of the prime (Bowman et al., 2006; Eimer and Schlaghecken, 2002; Schlaghecken et al., 2007; Schlaghecken and Eimer, 2006) or bias reversed by the mask (Lleras and Enns, 2004; Verleger et al., 2004) was introduced to explain the transition from positive to negative priming when SOA increases. Efforts were also made to reproduce positive and negative priming in computational models (Vorberg et al., 2003), neural network models (Bowman et al., 2006; Sohrabi and West,

2009), or computational models with biologically plausible neural implementations (Huber and O'Reilly, 2003).

The model we propose here does not necessarily conflict with previous theories, in the sense that priming effects are triggered by the prime and the mask (see the next section for more discussions on mask) and unfold over time. Neither is OTEM intended to be an exclusive explanation for priming effects: Some of the priming effects in the literature can only be explained by alternative accounts such as perceptual aftereffect (Fritsche et al., 2017; Klauer and Dittrich, 2010).

Almost all previous theories considered the visual priming effects as passively determined by the stimuli. Instead, OTEM implements the idea of active sensing (Lakatos et al., 2013, 2009, 2008; Schroeder et al., 2010; Zion Golumbic et al., 2013) and assumes that the perceptual system (1) rhythmically samples the congruent and incongruent, and (2) adaptively prepares for the prospective targets. This novel combination of attentional oscillation with temporal expectation enables OTEM to accommodate the recent empirical finding of oscillated priming as well as the classic effects.

Prior to OTEM, temporal expectation was not seriously considered in the literature of priming effects, though it has received growing attention in perception and memory (Nobre and van Ede, 2017). Consequently, previous priming theories might explain the decrease of RTs with increasing SOA (e.g. the nROUSE model of Huber and O'Reilly, 2003) but were unable to meanwhile account for the RT "jumps" with increasing SOA (Figure 3A). In contrast, with the introduction of temporal expectation—a concept that distinguishes SOA and temporal uncertainty, OTEM predicts both the observations.

OTEM also predicts that the classic priming effects may change with temporal context, since temporal expectations are learned from recent experience. As found in our new experiment, the magnitudes of positive and negative priming effects differed

481 across the four temporal expectation conditions: higher temporal uncertainty led to
482 smaller priming effects (Figure 3BC). Similarly, Naccache, Blandin, and Dehaene (2002)
483 found that the classic priming effects would vanish when the arrival time of the target
484 was barely predictable.

485 Our findings raise a general concern that the results of priming experiments
486 should be interpreted in their temporal contexts other than by individual SOAs. Some of
487 the previously found differences between priming experiments at the same SOAs might
488 be explained away by temporal contexts.

489 With all three priming effects arising from a common process, OTEM also
490 naturally predicts that positive and negative priming are closely related. In agreement
491 with this prediction, Boy and Sumner (2010) showed that both positive and negative
492 priming effects are proportional to the strength of stimulus-response associations: When
493 a novel stimulus-response mapping is used, it takes time to build associations, during
494 which positive and negative priming grow with time at the same pace.

495 In sum, OTEM reproduces both the classic and oscillated priming effects by
496 attributing the latter to instantaneous attentional fluctuations and the former to
497 accumulated biases driven by attentional oscillation and temporal expectation. By
498 explaining the classic priming effects as emergent properties of OTEM, we are not at
499 any position doubting the ecological significance of positive or negative priming.
500 Emergent properties of a system can be important by themselves, just like
501 consciousness is believed to be an emergent property of the brain (Minsky, 1986).
502

503 **Neurobiological motivations for OTEM**

504 OTEM is intended to capture the computational heuristics of the neural computations
505 underlying visual priming effects. The neurobiological motivations for some of its key

assumptions, such as attentional oscillation (VanRullen, 2016, 2013) and temporal expectation (de Lange et al., 2013; McGuire and Kable, 2013), have been specified in the Introduction. We describe the others below.

OTEM assumes a theta-band attentional oscillation whose phase is reset by the prime and the mask. Spontaneous theta-band neuronal oscillations are fairly common in the human brain and are readily reset by task-relevant stimuli (Rizzuto et al., 2003; Tesche and Karhu, 2000; see Buzsaki, 2006 for a review). Further, the oscillatory entrainment of sensory stimuli is anti-phased for the attended and unattended stimuli (Lakatos et al., 2013). Buzsaki (2006) suggested that theta-band neuronal oscillations serve as synchronizers to integrate information over time. Analogously, the attentional oscillation assumed in OTEM may help to integrate temporal expectations over time.

There have been elegant models (Huber and O'Reilly, 2003) on how positive priming may spontaneously transition into negative priming with increased exposure to the prime. For the visual (arrow) priming tasks we treated here, however, negative priming can hardly be explained solely as an effect of the prime, because negative priming effect has seldom been observed in unmasked priming tasks (Huang et al., 2015; Jaśkowski et al., 2008; Klotz and Wolff, 1995; Vorberg et al., 2003; but see Klauer and Dittrich, 2010 for an exception). Moreover, it has been found that negative priming would be weaker (Schlaghecken and Eimer, 2006) or even be absent (Jaśkowski and Przekoracka-Krawczyk, 2005; Lleras and Enns, 2006; Verleger et al., 2004) unless the mask shares visual features with the prime (see the arrow-shaped mask in Figure 1F for an example). In other words, masks are not passive stimuli that simply render the prime invisible but play an active role in the priming effects.

A mask that contains features of the prime, according to Huber (2008), will induce neural habituation to the prime and highlight the opposite features. Similar ideas have been expressed by Lleras and Enns (2004) in the object updating theory and are

analogous to perceptual aftereffect (Webster, 2015). We therefore assume that the mask, like the prime, resets the attentional oscillation but to a different phase that favors more of the opposite features. To capture potential individual differences, the exact phase reset by the mask is left to be a free parameter in OTEM, which turned out to be highly consistent in all our masked priming experiments and was anti-phased to that of the prime (Figure 1K and Figure 3D). That is, the mask effectively reverses the attentional oscillation set earlier by the prime.

Temporal discounting has been found in human perception and action (Shadmehr et al., 2010) as well as in economic decision-making (Frederick et al., 2002; Kable and Glimcher, 2007). In OTEM, we introduced temporal discounting to characterize the tendency to prepare more intensely for a near-future target compared to a far-future target that is equally likely to occur. When the discounting rate is zero, any future event would be treated as urgent as the present event and temporal expectation would thus be meaningless. On the other extreme, when the discounting rate is infinity, only the present matters, which is effectively the assumption adopted by many previous models including but not limited to the hazard rate model of temporal expectation (Los et al., 2014; Los and Van Den Heuvel, 2001; Luce, 1986; Niemi and Näätänen, 1981; Nobre et al., 2007).

Similar to previous studies on temporal expectation (Bueti et al., 2010; Janssen and Shadlen, 2005; Sharma et al., 2014), we also considered the participant's temporal uncertainty and used Weber's law (Allan, 2001; Gibbon, 1977) to model it, with the Weber fraction parameter set to be a constant estimated from previous research (Jazayeri and Shadlen, 2010). In the presence of temporal uncertainty, the probability of a future event can leak into the present such that the participant would appear to prepare for the future even if she only cared about the hazard rate at the current moment. At first sight, temporal uncertainty seems to play a role interchangeable with

temporal discounting, which renders the latter redundant. However, a model with the former alone would predict an increase of RT with increasing temporal uncertainty, other things being the same (Tsunoda and Kakei, 2011), which is opposite to our empirical finding that, in the 20-, 10-, or 4-SOA condition, blocks with longer SOAs tend to have shorter RTs (Figure 3A), though longer SOAs correspond to larger temporal uncertainty. Therefore, for both theoretical and practical reasons, we chose to include both temporal uncertainty and temporal discounting in OTEM.

OTEM assumes that two threads of perceptual or motor preparations develop in parallel before target onset. Simultaneous preparation for multiple potential actions has been reported in neuronal activities (Cisek, 2007, 2005; Cisek and Kalaska, 2010). Such pre-target preparing activities are largely driven by temporal expectation and can bias the subsequent actions (de Lange et al., 2013; Donner et al., 2009). According to OTEM, visual priming effects in RT arise from pre-target preparation instead of post-target decision (but also see the extended OTEM). It echoes the findings that attentional status (Nunez et al., 2017) or temporal expectation (Jepma et al., 2012) mostly influences the non-decision time instead of decision time in RT.

To avoid introducing too many degrees of freedom into OTEM, some of our assumptions were simplifying. For example, we assumed a transition from oscillatory dynamics to constant preparedness accumulation for the realized target immediately after target onset. To assume a delayed transition would be more realistic, since it takes time to detect the target. Given that the target appears at central vision with high contrast, such a delay tends to be negligible and whether to include it or not should have little influence on our conclusions.

Limitations and future directions

Visual priming tasks have various forms: The prime and target are often but not confined to arrows (Bar and Biederman, 1998; Boy and Sumner, 2010; Del Cul et al., 2007; Kiefer and Brendel, 2006; Klotz and Wolff, 1995); the response is typically key press (Bar and Biederman, 1998; Dehaene et al., 1998; Eimer and Schlaghecken, 1998; Jaśkowski et al., 2008), but can also be finger pointing (Schmidt, 2002), foot stepping (Eimer et al., 2002), eye movement (Sereno, 1995) or speech (Ansorge et al., 1998). In theory, OTEM can apply to all these tasks.

That being said, we does not intend to explain all important aspects of visual priming effects, such as how the strength of priming effects is influenced by the features of the prime and target, which has received elegant treatment in other models (Huber and O'Reilly, 2003; Kruijne and Meeter, 2017). Neither do we claim that our model provides an implementation-level explanation for visual priming effects. Our work, in Marr's (1982) term, is between the computational and algorithm levels based on neurobiologically motivated assumptions.

What OTEM provides are computational heuristics about how one common process may give rise to priming effects with various temporal dynamics, which allow us to make quantitative, testable behavioral predictions. Given that OTEM explains both the classic and oscillated priming effects based on attentional oscillation, a future test would be to directly manipulate attentional oscillation and see what happens to the priming effects. OTEM also predicts how a set of latent variables—temporal gain, attentional gain, and preparedness—may change between and within trials. This would facilitate model-based searches to further understand the neural basis of visual priming.

A coexistence of sustained and oscillated effects has also been found in spatial cueing tasks (see Introduction). More generally, OTEM offers a new perspective that may unify the attention-related classic findings with the increasing evidence for

attentional oscillations in visual perception. One future question is, may other attention-related classic phenomena be explained in a similar framework?

Methods

Experiments

We had analyzed data from two published experiments of Huang et al. (2015) and one new experiment (see Results). The experiments had been approved by the ethics committees of Institute of Biophysics at Chinese Academy of Sciences (#2006-IRB-005) and School of Psychological and Cognitive Sciences at Peking University (#2015-03-13c). All participants provided informed consent before the experiment and were paid for their time. Sixty-four young adults (29 male, aged 19–27) participated in the new experiment, with 16 participants randomly assigned to each of the four conditions. No statistical methods were used to predetermine sample sizes but our choice of sample size was based on previous work, including Huang et al. (2015). Time-out trials or trials with premature responses were excluded.

Statistical Analyses

We followed the methods of Huang et al. (2015) to decompose raw RTs into slow trends and detrended RTs. For each participant and separately for the congruent and incongruent, we smoothed raw RTs using a 240-msec moving window over SOA (implemented by MATLAB function *filtfilt*) to obtain slow trends. Subtracting slow trends from raw RTs resulted in detrended RTs. For spectral analysis, detrending was also performed using 4-degree polynomial fits.

To confirm that the theta-band oscillations observed in Huang et al. (2015) were not artifacts from the moving-window detrending method, we also smoothed raw RTs using exponential fits, whose results were presented in Figure 1-figure supplements 2 and 3. Different detrending methods led to similar results.

Fast Fourier Transform (FFT, implemented by MATLAB function *fft*) was used for spectral analysis. The permutation procedure and multiple-comparison correction method of Huang et al. (2015) were performed to test the statistical significance of the amplitude spectrum of detrended RTs as follows, separately for the congruent and incongruent. We generated surrogate signals by randomly shuffling the detrended RTs across SOAs within each participant, applied FFT to these surrogate signals, and computed the mean amplitude spectrum across participants. This procedure was repeated for 1,000 times to produce a distribution of mean amplitude at each frequency point, from which we elicited the uncorrected $p < 0.05$ threshold for false positives. To correct for multiple comparisons, we set the maximum of the uncorrected thresholds across frequency points as the corrected $p < 0.05$ threshold (Nichols and Holmes, 2002; Song et al., 2014).

As in Huang et al. (2015), the theta-band phase difference between the congruent and incongruent was calculated for each participant as the mean phase difference across 3–5 Hz. Rayleigh tests were used to test the phase coherence across participants. Statistical tests and averaging on circular variables were implemented by Matlab toolbox CircStat (Berens, 2009).

Oscillated temporal expectation model (OTEM)

<u>Preparedness accumulation</u>. We assume that two threads of preparedness are accumulated in parallel for the two potential targets after the prime and before target onset, each of which can be formulated as:

$$\frac{de_{\mathrm{alt},m}(t)}{dt} = \varphi_{\mathrm{alt}}(t)\rho_m(t) - \mu \ , \tag{1}$$

where alt denotes whether the potential target is congruent (C) or incongruent (IC) with

the prime, $\boldsymbol{m}$ denotes trial number, $\boldsymbol{t}$ denotes the delay since prime, $\boldsymbol{e_{alt,m}(t)}$ denotes accumulated preparedness, $\boldsymbol{\varphi_{alt}(t)}$ denotes attentional gain, $\boldsymbol{\rho_m(t)}$ denotes temporal gain, $\boldsymbol{\mu}$ is a leaky rate parameter.

We assume $e_{\mathrm{alt},m}(0) = 0$. To avoid premature responses before target onset, an upper boundary is imposed on $e_{\mathrm{alt},m}(0) = 0$. After the target arrives, the preparedness for the target continues to accumulate at a constant rate v while the other thread stops. The expected RT for Trial m is the duration from target onset ($\tau_{\mathrm{target},m}$) to the moment the preparedness hits the response threshold b :

$$x_{\mathrm{expt},m} = \frac{b - e_{\mathrm{alt},m}\left(\tau_{\mathrm{target},m}\right)}{v} \quad . \tag{2}$$

The observed RT $x_{\mathrm{obs},m}$ is modeled by adding a log-normal noise:

$$\log x_{\mathrm{obs},m} = \log x_{\mathrm{expt},m} + N\left(0, \sigma^2_{\mathrm{noise}}\right). \tag{3}$$

<u>Attentional gain</u>. We assume that the attentional gains for the two alternative targets add up to 2 and oscillate anti-phased over time, with the amplitude of oscillation decaying exponentially with time (Figure 2CD). We define

$$\psi(t) = \begin{cases} \exp\left(-\kappa t\right)\sin\left(2f\pi t + \theta_{\mathrm{prime}}\right), & t < \tau_{\mathrm{mask}}, \\ \exp\left(-\kappa t\right)\sin\left(2f\pi\left(t - \tau_{\mathrm{mask}}\right) + \theta_{\mathrm{mask}}\right), & t \geq \tau_{\mathrm{mask}} \end{cases} \tag{4}$$

where κ is a free parameter for decaying rate, f denotes the frequency of attentional oscillation, θ_{prime} and θ_{mask} are free parameters for phases reset by the prime and mask, τ_{mask} denotes the delay of mask. For the unmasked priming task, $\tau_{\mathrm{mask}} \to \infty$. (In the current implementation of OTEM, we defined $t = 0$ and τ_{mask} as the offset times of the prime and mask.) Following the finding that oscillated priming peaks at 3.3 Hz (Huang et al., 2015), we set $f = 3.3$.

The attentional gains for C and IC can be written as

$$\begin{aligned} \varphi_{\mathrm{C}}(t) &= \quad \psi(t)+1, \\ \varphi_{\mathrm{IC}}(t) &= \quad -\psi(t)+1. \end{aligned} \tag{5}$$

<u>Temporal gain: trial-by-trial learning</u>. We assume that the participant's temporal expectation for the target is learned from previous experience trial by trial (Figure 2A) following the delta-rule learning (Rescorla and Wagner, 1972):

$$p_m = p_{m-1} + \alpha\left(p'_{m-1} - p_{m-1}\right), \tag{6}$$

where p_m and p_{m-1} denote the expected distribution of τ_{target} at the beginning of Trial m and $m-1$, $0 \le \alpha \le 1$ is a free parameter for learning rate. The p'_{m-1} denotes the perceived distribution of τ_{target} on Trial $m-1$, which is a Gaussian distribution around $\tau_{\text{target},m-1}$:

$$p'_{m-1}(t) = \frac{1}{\sqrt{2\pi}\sigma_{\text{Weber}}} \exp\left(-\frac{\left(t-\tau_{\text{target},m-1}\right)^2}{2\sigma_{\text{Weber}}^2}\right), \tag{7}$$

where σ_{Weber} follows Weber's law, $\sigma_{\text{Weber}} = k\tau_{\text{target},m}$ for unmasked and $\sigma_{\text{Weber}} = k\left(\tau_{\text{target},m} - \tau_{\text{mask}}\right)$ for masked priming tasks, with Weber's fraction $k = 0.13$ (Jazayeri and Shadlen, 2010). We set p_1 to be a uniform distribution between the minimum and maximum τ_{target}.

<u>Temporal gain: real-time updating within trial</u>. We assume that within each trial the brain keeps updating its expectation for the arrival time of the target (Figure 2B). On Trial m, the expected distribution of τ_{target} at Time t ($t < \tau_{\text{target},m}$) is

$$q_m\left(t'\middle|t\right)=\begin{cases} 0, & t'<t, \\ \dfrac{p_m\left(t'\right)}{\int_t^{\infty} p_m\left(u\right)du}, & t'\geq t. \end{cases} \tag{8}$$

As a special case, the hazard rate of target onset at Time t is $h\left(t\right)=q_m\left(t'=t\middle|t\right)$.

Considering the target as a future reward, we define the temporal gain at Time t as the expectation of the discounted future reward:

$$\rho_m(t)=\int_t^{\infty}\gamma^{u-t}q_m(u|t)du\,, \tag{9}$$

where $0\leq\gamma\leq 1$ is a free parameter for discounting rate.

In total, OTEM has nine parameters for unmasked priming tasks: learning rate, α; temporal discounting rate, γ; leaky rate, μ; decaying rate of oscillation, κ; phase reset by the prime,θ_{prime}; maximum preparedness before target onset, ζ; accumulating rate after target onset, ν; responding threshold, b; standard deviation of log-normal noise, σ_{noise}. For masked priming tasks, there is one more parameter: phase reset by the mask, θ_{mask}.

<u>Frequency of attentional oscillation</u>

In the model fitting, we had fixed the frequency of attentional oscillation to 3.3 Hz, the observed frequency of oscillated priming. The RTs predicted by OTEM exhibits the same frequency of oscillated priming as that of the assumed attentional oscillation (Figure 1-figure supplement 1, Figure 3-figure supplements 1 and 2). That is, a theta-band attentional oscillation is sufficient for producing the theta-band oscillated priming.

We also tested whether the 3.3 Hz attentional oscillation is necessary. To do this, we varied the frequency of attentional oscillation, fit the OTEM model for each frequency, and compared their goodness-of-fit (AICc). For computational difficulties, we only considered a limited set of frequencies spanning 2 to 16 Hz. For all three experiments,

720 the AICc first decreased and later increased with the frequency of attentional oscillated,
721 with the best fit occurred at 3.3 or 4 Hz (Figure 2-figure supplement 2).

722 **Extension of OTEM with a decision process**

723 To explain the patterned errors in visual priming tasks, we enhanced OTEM with an
724 error-prone decision process. The extended OTEM assumes that after target onset both
725 the congruent and incongruent threads continue to accumulate, inhibiting each other and
726 racing to the responding bound. The racing follows a noise-free version of the leaky
727 competing accumulator model (Usher and McClelland, 2001):

728
$$\begin{cases} \dfrac{de_{\text{target},m}}{dt} = & v_{\text{target}} - \eta e_{\text{other},m}, \\ \dfrac{de_{\text{other},m}}{dt} = & v_{\text{other}} - \eta e_{\text{target},m}. \end{cases} \tag{10}$$

729 where η is a free parameter, v_{target} and v_{other} are accumulating rates for the target and
730 the other threads. The values of v_{target} and v_{other} on each trial are randomly sampled
731 from Gaussian distributions $N\left(\bar{v}_{\text{target}}, \sigma^2_{\text{target}}\right)$ and $N\left(\bar{v}_{\text{other}}, \sigma^2_{\text{other}}\right)$, with $\bar{v}_{\text{target}} > \bar{v}_{\text{other}}$.

732 Due to computational difficulties, we did not fit the extended OTEM and focused
733 on qualitative predictions. To simulate for the results of Vorberg et al. (2003), we used
734 the fitted parameters from the 4-SOA condition and manually set the additional
735 parameters for the decision process.

736

737 **Oscillated urgency model**

738 The oscillated urgency model is the same as OTEM, except that the preparedness for a
739 potential target is not accumulated over time but determined by hazard rate. That is, Eq.
740 1 is replaced by

$$e_{\mathrm{alt},m} = \varphi_{\mathrm{alt}}(t) h_m(t), \tag{11}$$

where $\varphi_{\mathrm{alt}}(t)$ denotes attentional gain, $h_m(t)$ denotes hazard rate.

In total, oscillated urgency model has 7 free parameters: learning rate, α; decaying rate of oscillation, κ; phase reset by the prime or mask, θ; maximum preparedness before target onset, ζ; accumulating rate after target onset, ν; response threshold, b; standard deviation of log-normal noise, σ_{noise}.

Constant accumulation model

The constant accumulation model is based on the accumulator model of Vorberg et al. (2003). The model assumes two accumulators for the two potential targets, the congruent and incongruent. Response is made when the absolute difference between the two accumulators exceeds the response threshold b. The same log-normal noise applies as in OTEM (Eq. 3).

Each accumulator follows

$$\frac{de_{\mathrm{alt},m}(t)}{dt} = -\mu e_{\mathrm{alt},m}(t) + \lambda_{\mathrm{alt}}(t), \tag{12}$$

where μ is a free parameter for growth-decay rate, $\lambda_{\mathrm{alt}}(t)$ denotes the rate of accumulation triggered by the prime, mask, or target as defined below. Following Vorberg et al. (2003), we assume that the prime and target would trigger positive accumulation rates for accumulators in their directions. To account for the observed effect of the mask (i.e. negative priming in masked priming tasks), we further assume that the mask would trigger a negative accumulation rate for the accumulator in the direction of the prime. That is, when the target is congruent with the prime,

$$\begin{aligned}\lambda_{\mathrm{C}}(t) &= \begin{cases}\lambda_s, & 0 \le t < \tau_{\mathrm{mask}}, \\ -\lambda_s, & \tau_{\mathrm{mask}} \le t < \tau_{\mathrm{target},m}, \\ \lambda_s, & \tau_{\mathrm{target},m} \le t,\end{cases} \\ \lambda_{\mathrm{IC}}(t) &= 0.\end{aligned} \tag{13}$$

When the target is incongruent with the prime,

$$\begin{aligned}\lambda_{\mathrm{C}}(t) &= \begin{cases}\lambda_s, & 0 \le t < \tau_{\mathrm{mask}}, \\ -\lambda_s, & \tau_{\mathrm{mask}} \le t < \tau_{\mathrm{target},m}, \\ 0, & \tau_{\mathrm{target},m} \le t,\end{cases} \\ \lambda_{\mathrm{IC}}(t) &= \begin{cases}0, & t < \tau_{\mathrm{target},m}, \\ \lambda_s, & \tau_{\mathrm{target},m} \le t.\end{cases}\end{aligned} \tag{14}$$

where λ_s is a free parameter, $t = 0$ corresponds to prime onset and τ_{mask} to mask onset. For the unmasked condition, $\tau_{\mathrm{mask}} = \tau_{\mathrm{target},m}$.

The threshold parameter b is redundant and fixed as 1. In total, the model has 4 free parameters: effect of stimulus, λ_s; growth-decay rate, μ; maximum preparedness before target, ζ; standard deviation of log-normal noise, σ_{noise}.

Model fitting and comparison procedures

All the models were fitted on the individual level using the maximum likelihood estimate. We used the interior-point algorithm of the *fmincon* function in MATLAB (MathWorks) to find the parameters that minimized negative log likelihood. To verify that we had found the global minimum, we repeated the search process with different starting points. We used AICc—the Akaike information criterion with a correction for finite sample size (Akaike, 1974; Hurvich and Tsai, 1989)—for model comparison and calculated the protected exceedance probability of the group-level Bayesian model selection (Rigoux et al., 2014; Stephan et al., 2009) as an omnibus measure across participants.

Data availability

All data and codes are available for download at https://osf.io/69by5/ .

References

Akaike H. 1974. A new look at the statistical model identification. *IEEE transactions on automatic control* **19**:716–723. doi:10.1007/978-1-4612-1694-0_16

Allan LG. 2001. Time Perception Models In: Smelser NJ, Baltes PB, editors. International Encyclopedia of the Social & Behavioral Sciences: Second Edition. Oxford: Elsevier. pp. 15696–15699. doi:10.1016/B0-08-043076-7/00668-9

Ansorge U, Klotz W, Neumann O. 1998. Manual and verbal responses to completely masked (unreportable) stimuli: Exploring some conditions for the metacontrast dissociation. *Perception* **27**:1177–1189. doi:10.1068/p271177

Bar M, Biederman I. 1998. Subliminal visual priming. *Psychological Science* **9**:464–469. doi:10.1111/1467-9280.00086

Benedetto A, Morrone MC. 2017. Saccadic suppression is embedded within extended oscillatory modulation of sensitivity. *Journal of Neuroscience* **37**:3661–3670. doi:10.1523/JNEUROSCI.2390-16.2016

Berens P. 2009. CircStat: A MATLAB Toolbox for Circular Statistics. *Journal of Statistical Software, Articles* **31**:1–21. doi:10.18637/jss.v031.i10

Bowman H, Schlaghecken F, Eimer M. 2006. A neural network model of inhibitory processes in subliminal priming. *Visual Cognition* **13**:401–480. doi:10.1080/13506280444000823

Boy F, Sumner P. 2010. Tight coupling between positive and reversed priming in the masked prime paradigm. *Journal of Experimental Psychology: Human Perception and Performance* **36**:892–905. doi:10.1037/a0017173

Bueti D, Bahrami B, Walsh V, Rees G. 2010. Encoding of Temporal Probabilities in the Human Brain. *The Journal of Neuroscience* **30**:4343–4352. doi:10.1523/JNEUROSCI.2254-09.2010

809 Buzsáki G. 2006. Rhythms of the Brain. New York: Oxford University Press.
810 doi:10.1093/acprof:oso/9780195301069.001.0001
811 Chen A, Wang A, Wang T, Tang X, Zhang M. 2017. Behavioral Oscillations in Visual
812 Attention Modulated by Task Difficulty. *Frontiers in Psychology* **8**:1630.
813 doi:10.3389/fpsyg.2017.01630
814 Cisek P. 2007. Cortical mechanisms of action selection: the affordance competition
815 hypothesis. *Philosophical transactions of the Royal Society of London Series B,*
816 *Biological sciences* **362**:1585–1599. doi:10.1098/rstb.2007.2054
817 Cisek P. 2005. Neural representations of motor plans, desired trajectories, and
818 controlled objects. *Cognitive Processing* **6**:15–24. doi:10.1007/s10339-004-0046-7
819 Cisek P, Kalaska JF. 2010. Neural Mechanisms for Interacting with a World Full of
820 Action Choices. *Annual Review of Neuroscience* **33**:269–298.
821 doi:10.1146/annurev.neuro.051508.135409
822 Damian MF. 2001. Congruity effects evoked by subliminally presented primes:
823 Automaticity rather than semantic processing. *Journal of Experimental Psychology:*
824 *Human Perception and Performance* **27**:154–165. doi:10.1037/0096-1523.27.1.154
825 de Lange FP, Rahnev DA, Donner TH, Lau H. 2013. Prestimulus Oscillatory Activity over
826 Motor Cortex Reflects Perceptual Expectations. *The Journal of Neuroscience*
827 **33**:1400–1410. doi:10.1523/JNEUROSCI.1094-12.2013
828 Dehaene S, Naccache L, Le Clec'H G, Koechlin E, Mueller M, Dehaene-Lambertz G,
829 van de Moortele P-F, Le Bihan D. 1998. Imaging unconscious semantic priming.
830 *Nature* **395**:597–600. doi:10.1038/26967
831 Del Cul A, Baillet S, Dehaene S. 2007. Brain Dynamics Underlying the Nonlinear
832 Threshold for Access to Consciousness. *PLOS Biology* **5**:e260.
833 doi:10.1371/journal.pbio.0050260

834 Donner TH, Siegel M, Fries P, Engel AK. 2009. Buildup of Choice-Predictive Activity in
835 Human Motor Cortex during Perceptual Decision Making. *Current Biology* **19**:1581–
836 1585. doi:10.1016/j.cub.2009.07.066
837 Eimer M. 1999. Facilitatory and inhibitory effects of masked prime stimuli on motor
838 activation and behavioural performance. *Acta psychologica* **101**:293–313.
839 doi:10.1016/S0001-6918(99)00009-8
840 Eimer M, Schlaghecken F. 2003. Response facilitation and inhibition in subliminal
841 priming. *Biological Pyschology* **64**:7–26. doi:10.1016/S0301-0511(03)00100-5
842 Eimer M, Schlaghecken F. 2002. Links between conscious awareness and response
843 inhibition: evidence from masked priming. *Psychonomic bulletin & review* **9**:514–
844 520. doi:10.3758/BF03196307
845 Eimer M, Schlaghecken F. 1998. Effects of Masked Stimuli on Motor Activation:
846 Behavioral and Electrophysiological Evidence. *Journal of experimental psychology*
847 *Human perception and performance* **24**:1737–1747. doi:10.1037/0096-
848 1523.24.6.1737
849 Eimer M, Schubö A, Schlaghecken F. 2002. Locus of inhibition in the masked priming of
850 response alternatives. *Journal of Motor Behavior* **34**:3–10.
851 doi:10.1080/00222890209601926
852 Fiebelkorn IC, Saalmann YB, Kastner S. 2013. Rhythmic sampling within and between
853 objects despite sustained attention at a cued location. *Current Biology* **23**:2553–
854 2558. doi:10.1016/j.cub.2013.10.063
855 Frederick S, Loewenstein G, O'Donoghue T. 2002. Time Discounting and Time
856 Preference: A Critical Review. *Journal of Economic Literature* **40**:351–401.
857 doi:10.1257/002205102320161311

Fritsche M, Mostert P, de Lange FP. 2017. Opposite Effects of Recent History on Perception and Decision. *Current Biology* **27**:590–595. doi:10.1016/j.cub.2017.01.006

Gibbon J. 1977. Scalar expectancy theory and Weber's law in animal timing. *Psychological Review* **84**:279–325. doi:10.1037/0033-295X.84.3.279

Huang Y, Chen L, Luo H. 2015. Behavioral Oscillation in Priming: Competing Perceptual Predictions Conveyed in Alternating Theta-Band Rhythms. *The Journal of Neuroscience* **35**:2830–2837. doi:10.1523/JNEUROSCI.4294-14.2015

Huber DE. 2014. The Rise and Fall of the Recent Past: A Unified Account of Immediate Repetition Paradigms In: Ross B, editor. Psychology of Learning and Motivation. Cambridge: Academic Press. pp. 191–226. doi:10.1016/B978-0-12-800090-8.00005-6

Huber DE. 2008. Immediate priming and cognitive aftereffects. *Journal of Experimental Psychology: General* **137**:324–347. doi:10.1037/0096-3445.137.2.324

Huber DE, O'Reilly RC. 2003. Persistence and accommodation in short-term priming and other perceptual paradigms: temporal segregation through synaptic depression. *Cognitive Science* **27**:403–430. doi:https://doi.org/10.1016/S0364-0213(03)00012-0

Hurvich CM, Tsai C-L. 1989. Regression and time series model selection in small samples. *Biometrika* **76**:297–307. doi:10.1093/biomet/76.2.297

Janssen P, Shadlen MN. 2005. A representation of the hazard rate of elapsed time in macaque area LIP. *Nature Neuroscience* **8**:234–241. doi:10.1038/nn1386

Jaśkowski P, Białuńska A, Tomanek M, Verleger R. 2008. Mask- and distractor-triggered inhibitory processes in the priming of motor responses: An EEG study. *Psychophysiology* **45**:70–85. doi:10.1111/j.1469-8986.2007.00595.x

Jaśkowski P, Przekoracka-Krawczyk A. 2005. On the role of mask structure in subliminal priming. *Acta Neurobiologiae Experimentalis* **65**:409–417.

Jazayeri M, Shadlen MN. 2010. Temporal context calibrates interval timing. *Nature neuroscience* **13**:1020–1026. doi:10.1038/nn.2590

Jepma M, Wagenmakers E-J, Nieuwenhuis S. 2012. Temporal expectation and information processing: A model-based analysis. *Cognition* **122**:426–441. doi:https://doi.org/10.1016/j.cognition.2011.11.014

Kable JW, Glimcher PW. 2007. The neural correlates of subjective value during intertemporal choice. *Nature Neuroscience* **10**:1625–1633. doi:10.1038/nn2007

Kiefer M, Brendel D. 2006. Attentional modulation of unconscious “automatic” processes: Evidence from event-related potentials in a masked priming paradigm. *Journal of Cognitive Neuroscience* **18**:184–198. doi:10.1162/jocn.2006.18.2.184

Kienitz R, Schmiedt JT, Shapcott KA, Kouroupaki K, Saunders RC, Schmid MC. 2018. Theta Rhythmic Neuronal Activity and Reaction Times Arising from Cortical Receptive Field Interactions during Distributed Attention. *Current Biology* **28**:2377–2387. doi:10.1016/j.cub.2018.05.086

Klauer KC, Dittrich K. 2010. From sunshine to double arrows: An evaluation window account of negative compatibility effects. *Journal of Experimental Psychology: General* **139**:490–519. doi:10.1037/a0019746

Klein RM. 2000. Inhibition of return. *Trends in Cognitive Sciences* **4**:138–147. doi:10.1016/S1364-6613(00)01452-2

Klotz W, Wolff P. 1995. The effect of a masked stimulus on the response to the masking stimulus. *Psychological Research* **58**:92–101. doi:10.1007/BF00571098

Kruijne W, Meeter M. 2017. You prime what you code: The fAIM model of priming of pop-out. *PLoS ONE*. doi:10.1371/journal.pone.0187556

908 Lakatos P, Karmos G, Mehta AD, Ulbert I, Schroeder CE. 2008. Entrainment of
909 Neuronal Oscillations as a Mechanism of Attentional Selection. *Science* **320**:110–
910 113. doi:10.1126/science.1154735
911 Lakatos P, Musacchia G, O'Connel MN, Falchier AY, Javitt DC, Schroeder CE. 2013.
912 The Spectrotemporal Filter Mechanism of Auditory Selective Attention. *Neuron*
913 **77**:750–761. doi:10.1016/j.neuron.2012.11.034
914 Lakatos P, O'Connell MN, Barczak A, Mills A, Javitt DC, Schroeder CE. 2009. The
915 Leading Sense: Supramodal Control of Neurophysiological Context by Attention.
916 *Neuron* **64**:419–430. doi:10.1016/j.neuron.2009.10.014
917 Landau AN, Fries P. 2012. Attention samples stimuli rhythmically. *Current Biology*
918 **22**:1000–1004. doi:10.1016/j.cub.2012.03.054
919 Landau AN, Schreyer HM, Van Pelt S, Fries P. 2015. Distributed attention is
920 implemented through theta-rhythmic gamma modulation Published in edited form
921 in: Current Biology. *Current Biology* **25**:2332–2337. doi:10.1016/j.cub.2015.07.048
922 Lingnau A, Vorberg D. 2005. The time course of response inhibition in masked priming.
923 *Perception and Psychophysics* **67**:545–557. doi:10.3758/BF03193330
924 Lleras A, Enns JT. 2006. How much like a target can a mask be? Geometric, spatial,
925 and temporal similarity in priming: a reply to Schlaghecken and Eimer (2006).
926 *Journal of experimental psychology General* **135**:495–500. doi:10.1037/0096-
927 3445.135.3.495
928 Lleras A, Enns JT. 2004. Negative Compatibility or Object Updating? A Cautionary Tale
929 of Mask-Dependent Priming. *Journal of Experimental Psychology: General*
930 **133**:475–493. doi:10.1037/0096-3445.133.4.475
931 Los SA, Kruijne W, Meeter M. 2014. Outlines of a multiple trace theory of temporal
932 preparation. *Frontiers in Psychology* **5**:1058. doi:10.3389/fpsyg.2014.01058

933 Los SA, Van Den Heuvel CE. 2001. Intentional and unintentional contributions to
934 nonspecific preparation during reaction time foreperiods. *Journal of Experimental*
935 *Psychology: Human Perception and Performance* **27**:370–386. doi:10.1037/0096-
936 1523.27.2.370
937 Luce RD. 1986. Response times: Their role in inferring elementary mental organization.
938 New York, NY: Oxford University Press.
939 Makeig S, Westerfield M, Jung T-P, Enghoff S, Townsend J, Courchesne E, Sejnowski
940 TJ. 2002. Dynamic Brain Sources of Visual Evoked Responses. *Science* **295**:690–
941 694. doi:10.1126/science.1066168
942 Marr D. 1982. Vision: A computational investigation into the human representation and
943 processing of visual information. Cambridge, MA: MIT Press.
944 Mattler U, Palmer S. 2012. Time course of free-choice priming effects explained by a
945 simple accumulator model. *Cognition* **123**:347–360.
946 doi:10.1016/j.cognition.2012.03.002
947 McCartney H, Johnson AD, Weil ZM, Givens B. 2004. Theta reset produces optimal
948 conditions for long-term potentiation. *Hippocampus* **14**:684–687.
949 doi:10.1002/hipo.20019
950 McGuire JT, Kable JW. 2013. Rational temporal predictions can underlie apparent
951 failures to delay gratification. *Psychological Review* **120**:395–410.
952 doi:10.1037/a0031910
953 Minsky M. 1986. The Society of Mind. New York, NY: Simon & Schuster, Inc.
954 Naccache L, Blandin E, Dehaene S. 2002. Unconscious Masked Priming Depends on
955 Temporal Attention. *Psychological Science* **13**:416–424. doi:10.1111/1467-
956 9280.00474
957 Neumann O, Klotz W. 1994. Motor responses to nonreportable, masked stimuli: Where
958 is the limit of direct parameter specification? In: Umiltà C, Moscovitch M, editors.

Attention and Performance XV, Attention and Performance Series. Cambridge, MA: MIT Press. pp. 123–150.

Nichols TE, Holmes AP. 2002. Nonparametric permutation tests for functional neuroimaging: A primer with examples. *Human Brain Mapping* **15**:1–25. doi:10.1002/hbm.1058

Niemi P, Näätänen R. 1981. Foreperiod and simple reaction time. *Psychological Bulletin* **89**:133–162. doi:10.1037/0033-2909.89.1.133

Nobre A, Correa A, Coull J. 2007. The hazards of time. *Current Opinion in Neurobiology* **17**:465–470. doi:10.1016/j.conb.2007.07.006

Nobre AC, Rohenkohl G. 2014. Time for the fourth dimension in attention In: Nobre AC, Kastner S, editors. The Oxford Handbook of Attention. Oxford, UK: Oxford University Press. pp. 676–721. doi:10.1093/oxfordhb/9780199675111.013.036

Nobre AC, van Ede F. 2017. Anticipated moments: temporal structure in attention. *Nature Reviews Neuroscience* **19**:34. doi:10.1038/nrn.2017.141

Nunez MD, Vandekerckhove J, Srinivasan R. 2017. How attention influences perceptual decision making: Single-trial EEG correlates of drift-diffusion model parameters. *Journal of Mathematical Psychology* **76**:117–130. doi:10.1016/j.jmp.2016.03.003

Posner MI, Cohen Y. 1984. Components of Visual Orienting In: Bouma H, Bouwhuis DG, editors. Attention and Performance X. Hillsdale, NJ: Lawrence Erlbaum Associates. pp. 531–556.

Praamstra P, Seiss E. 2005. The neurophysiology of response competition: motor cortex activation and inhibition following subliminal response priming. *Journal of cognitive neuroscience* **17**:483–493. doi:10.1162/0898929053279513

Rescorla RA, Wagner AR. 1972. A theory of Pavlovian conditioning: Variations in the effectiveness of reinforcement and nonreinforcement In: Black AH, Prokasy WF,

editors. Classical Conditioning II: Current Research and Theory. East Norwalk, CT: Appleton-Century-Crofts. pp. 64–99.

Rigoux L, Stephan KE, Friston KJ, Daunizeau J. 2014. Bayesian model selection for group studies — Revisited. *Neuroimage* **84**:971–985. doi:10.1016/j.neuroimage.2013.08.065

Rizzuto DS, Madsen JR, Bromfield EB, Schulze-Bonhage A, Seelig D, Aschenbrenner-Scheibe R, Kahana MJ. 2003. Reset of human neocortical oscillations during a working memory task. *Proceedings of the National Academy of Sciences* **100**:7931–7936. doi:10.1073/pnas.0732061100

Sack AT, van der Mark S, Schuhmann T, Schwarzbach J, Goebel R. 2009. Symbolic action priming relies on intact neural transmission along the retino-geniculo-striate pathway. *Neuroimage* **44**:284–293. doi:10.1016/j.neuroimage.2008.07.030

Schacter DL, Buckner RL. 1998. Priming and the Brain. *Neuron* **20**:185–195. doi:10.1016/S0896-6273(00)80448-1

Schlaghecken F, Eimer M. 2006. Active masks and active inhibition: A comment on Lleras and Enns (2004) and on Verleger, Jaśkowski, Aydemir, van der Lubbe, and Groen (2004). *Journal of Experimental Psychology: General* **135**:484–494. doi:10.1037/0096-3445.135.3.484

Schlaghecken F, Eimer M. 2002. Motor activation with and without inhibition: Evidence for a threshold mechanism in motor control. *Perception & Psychophysics* **64**:148–162. doi:10.3758/BF03194564

Schlaghecken F, Rowley L, Sembi S, Simmons R, Whitcomb D. 2007. The negative compatibility effect: A case for self-inhibition. *Advances in Cognitive Psychology* **3**:227–240. doi:10.2478/v10053-008-0027-y

Schmidt T. 2002. The Finger in Flight: Real-Time Motor Control by Visually Masked Color Stimuli. *Psychological Science* **13**:112–118. doi:10.1111/1467-9280.00421

Schroeder CE, Wilson DA, Radman T, Scharfman H, Lakatos P. 2010. Dynamics of Active Sensing and perceptual selection. *Current Opinion in Neurobiology* **20**:172–176. doi:https://doi.org/10.1016/j.conb.2010.02.010

Sereno SC. 1995. Resolution of lexical ambiguity: Evidence from an eye movement priming paradigm. *Journal of Experimental Psychology: Learning, Memory, and Cognition*. doi:10.1037/0278-7393.21.3.582

Shadmehr R, Orban de Xivry JJ, Xu-Wilson M, Shih T-Y. 2010. Temporal Discounting of Reward and the Cost of Time in Motor Control. *The Journal of Neuroscience* **30**:10507–10516. doi:10.1523/JNEUROSCI.1343-10.2010

Sharma J, Sugihara H, Katz Y, Schummers J, Tenenbaum J, Sur M. 2014. Spatial Attention and Temporal Expectation Under Timed Uncertainty Predictably Modulate Neuronal Responses in Monkey V1. *Cerebral Cortex* **25**:2894–2906. doi:10.1093/cercor/bhu086

Sohrabi A, West RL. 2009. Positive and negative congruency effects in masked priming: A neuro-computational model based on representation, attention, and conflict. *Brain Research* **1289**:124–132. doi:10.1016/j.brainres.2009.07.004

Song K, Meng M, Chen L, Zhou K, Luo H. 2014. Behavioral Oscillations in Attention: Rhythmic α Pulses Mediated through θ Band. *Journal of Neuroscience* **34**:4837–4844. doi:10.1523/JNEUROSCI.4856-13.2014

Stephan KE, Penny WD, Daunizeau J, Moran RJ, Friston KJ. 2009. Bayesian model selection for group studies. *Neuroimage* **46**:1004–1017. doi:10.1016/j.neuroimage.2009.03.025

Summerfield C, de Lange FP. 2014. Expectation in perceptual decision making: neural and computational mechanisms. *Nature Reviews Neuroscience* **15**:745–756. doi:10.1038/nrn3838

Sumner P. 2007. Negative and positive masked-priming – implications for motor inhibition. *Advances in Cognitive Psychology* **3**:317–326. doi:10.2478/v10053-008-0033-0

Sutton RS, Barto AG. 1998. Introduction to reinforcement learning. Cambridge, MA: MIT Press.

Tesche CD, Karhu J. 2000. Theta oscillations index human hippocampal activation during a working memory task. *Proceedings of the National Academy of Sciences* **97**:919–924. doi:10.1073/pnas.97.2.919

Tomassini A, Spinelli D, Jacono M, Sandini G, Morrone MC. 2015. Rhythmic Oscillations of Visual Contrast Sensitivity Synchronized with Action. *Journal of Neuroscience* **35**:7019–7029. doi:10.1523/JNEUROSCI.4568-14.2015

Tsunoda Y, Kakei S. 2011. Anticipation of future events improves the ability to estimate elapsed time. *Experimental Brain Research* **214**:323–334. doi:10.1007/s00221-011-2821-x

Tulving E, Schacter DL. 1990. Priming and human memory systems. *Science* **247**:301–306. doi:10.1126/science.2296719

Usher M, McClelland JL. 2001. The time course of perceptual choice: The leaky, competing accumulator model. *Psychological Review*. doi:10.1037/0033-295X.108.3.550

van Vugt M, Simen P, Nystrom L, Holmes P, Cohen J. 2012. EEG Oscillations Reveal Neural Correlates of Evidence Accumulation. *Frontiers in Neuroscience* **6**:106. doi:10.3389/fnins.2012.00106

VanRullen R. 2016. Perceptual Cycles. *Trends in cognitive sciences* **20**:1–6.

VanRullen R. 2013. Visual attention: A rhythmic process? *Current Biology* **23**:R1110–R1112. doi:10.1016/j.cub.2013.11.006

Verleger R, Jaśkowski P, Aydemir A, van der Lubbe RHJ, Groen M. 2004. Qualitative differences between conscious and nonconscious processing? On inverse priming induced by masked arrows. *Journal of Experimental Psychology: General* **133**:494–515. doi:10.1037/0096-3445.133.4.494

Vorberg D, Mattler U, Heinecke A, Schmidt T, Schwarzbach J. 2003. Different time courses for visual perception and action priming. *Proceedings of the National Academy of Sciences* **100**:6275–6280. doi:10.1073/pnas.0931489100

Webster MA. 2015. Visual Adaptation. *Annual Review of Vision Science* **1**:547–567. doi:10.1146/annurev-vision-082114-035509

Wutz A, Muschter E, van Koningsbruggen MG, Weisz N, Melcher D. 2016. Temporal integration windows in neural processing and perception aligned to saccadic eye movements. *Current Biology* **26**:1659–1668. doi:10.1016/j.cub.2016.04.070

Zion Golumbic EM, Ding N, Bickel S, Lakatos P, Schevon CA, McKhann GM, Goodman RR, Emerson R, Mehta AD, Simon JZ. 2013. Mechanisms underlying selective neuronal tracking of attended speech at a “cocktail party.” *Neuron* **77**:980–991. doi:10.1016/j.neuron.2012.12.037

Figure supplements

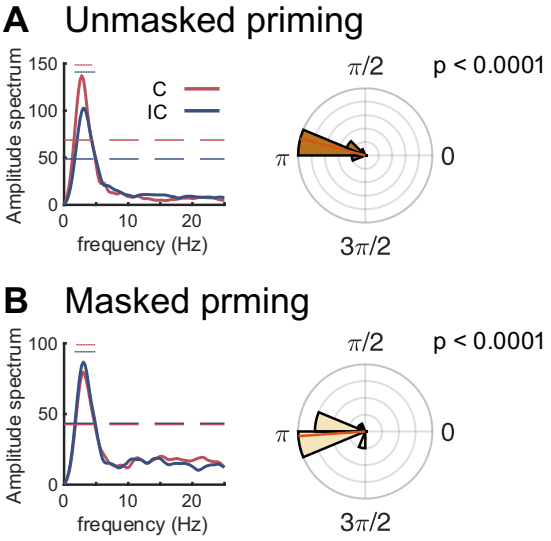

Figure 1-figure supplement 1. Spectral analysis of the detrended RT from the OTEM fits for the unmasked (A) and masked (B) priming tasks of Huang et al. (2015). We submitted the RTs by OTEM to the spectral analysis method of Huang et al. (2015) and presented the results in a similar way as the real data. Left panels: amplitude spectrum, separately for the congruent (red curve) and incongruent (blue curve). Dash lines denote the 0.05 significance threshold of permutation test (corrected for multiple comparisons). Significant frequency points are marked by dots above the spectrum curves. Right panels: phase difference between the congruent and incongruent in theta-band oscillation (3–5 Hz). Rose plot shows the distribution of phase differences across participants, with the mean phase difference marked by a red line. The *p* value refers to the result of Rayleigh test on coherence. For the detrended RT, the OTEM fits captured the theta-band oscillation of the real data in both the amplitude spectrum and the anti-phase between the congruent and incongruent. See Methods and Huang et al. (2015) for the spectral analysis method and the results of real data.

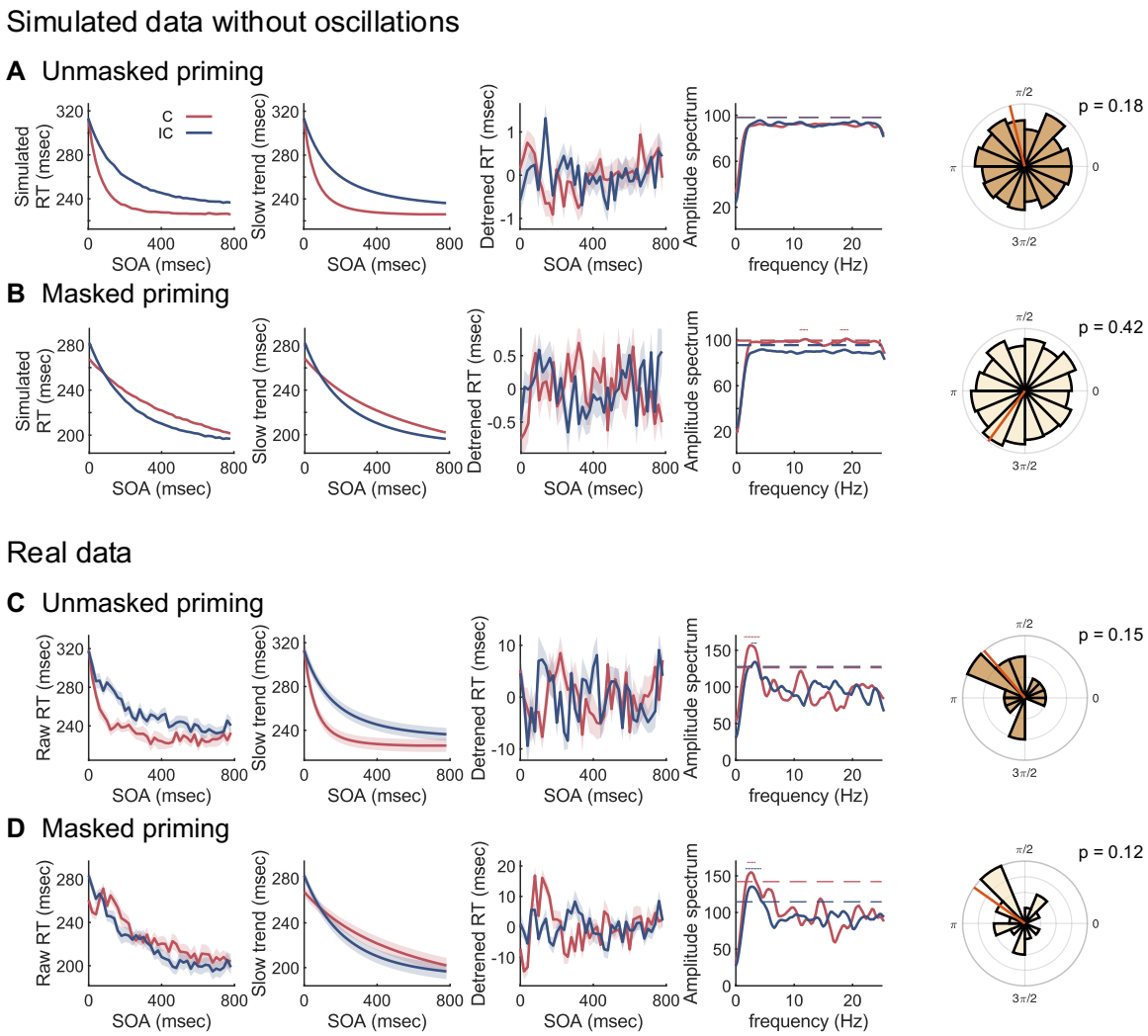

Figure 1-figure supplement 2. Oscillated priming effects found in Huang et al. (2015) are unlikely to be artifacts from detrending methods. To exclude the possibility that the oscillated priming effects found in Huang et al. (2015) were artifacts from detrending methods, we applied a different detrending method—exponential curve fitting—to simulated data without oscillations (**A**, **B**) and to the real data (**C**, **D**). Slow trends were computed by fitting an exponential curve to the raw RT curve. The detrended RT was then submitted to Fourier transforms. The simulated data without oscillations were generated by adding Gaussian white noises to the slow trends extracted from individuals participants' RT curves (separately for the congruent and incongruent). Each participant's slow trends were used in 100 times of data generation, resulting in a dataset of 1600 (unmasked priming) or 1800 (masked priming) simulated participants. Columns from left to right are plots respectively for the raw RT, slow trend (exponential curve),

detrended RT, amplitude spectrum of detrended RT, and the phase difference between the congruent and incongruent in theta-band. Conventions follow **Figure 1** and **Figure 1-figure supplement 1**. For the simulated data without oscillations (**A**, unmasked priming; **B**, masked priming), there not no above-chance oscillations, indicating that the exponential curve fitting would not introduce artifacts for exponentially decreasing RTs. In contrast, theta-band oscillations were still identified in the real data (**C**, unmasked priming; **D**, masked priming).

Removing SOAs before 200 msec

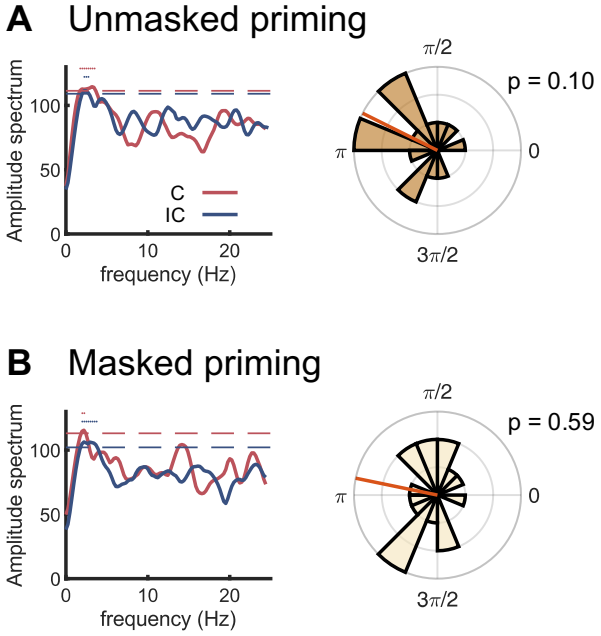

Figure 1-figure supplement 3. Evidence for an ongoing oscillation instead of just one beat in the detrended RT of Huang et al. (2015). To exclude the possibility that the theta-band power detected in the detrended RT (Figure 1-figure supplement 2CD) may simply come from a single beat in the first 200 msec, we removed SOAs before 200 msec and submitted the truncated detrended RT curve to Fourier transforms. Detrending and spectral analysis methods were the same as those used for Figure 1-figure supplement 2. The resulting theta-band power remained statistically significant for both the unmasked priming (**A**) and masked priming (**B**), and for both the congruent and incongruent. The mean phase difference between the congruent and incongruent was still close to π, though the phase coherence failed to reach significance, probably due to reduced statistical power in the truncated data. Conventions follow **Figure 1-figure supplement 1**.

Figure 2-figure supplement 1. How OTEM predictions vary with model parameters. We used OTEM with different parameter values to generate simulated RT as a function of SOA for the congruent (red) and incongruent (blue). **Left**: unmasked priming. **Right**: masked priming. Default parameter values: $\theta_{\text{prime}} = 0$, $\theta_{\text{mask}} = \pi$, $\alpha = 0.5$, $\gamma = 0.8$, $\mu = 0.6$, $\kappa = 9$, $\zeta = 160$, $\nu = 3600$, $b = 1000$, $\sigma_{\text{noise}} = 0.2$. For the simulation of each panel, we replaced the default parameter with the parameter labeled above the panel. We divided all parameters into two categories (**A** and **B**) based on whether they can lead to qualitative changes in the classic priming effects. The simulated results of each parameter is presented on a separate row. **A**,

phase reset parameters θ_{prime} and θ_{mask}, whose values determine whether there are sustained positive priming or negative priming. **B**, the remaining parameters, whose values have little influence on the qualitative features of the priming effects. To summarize, though OTEM has up to 10 free parameters, only 2 parameters are key to its qualitative predictions. In other words, the model's capability to capture various priming effects is more likely due to its internal structure instead of due to the flexibility from excessive parameters.

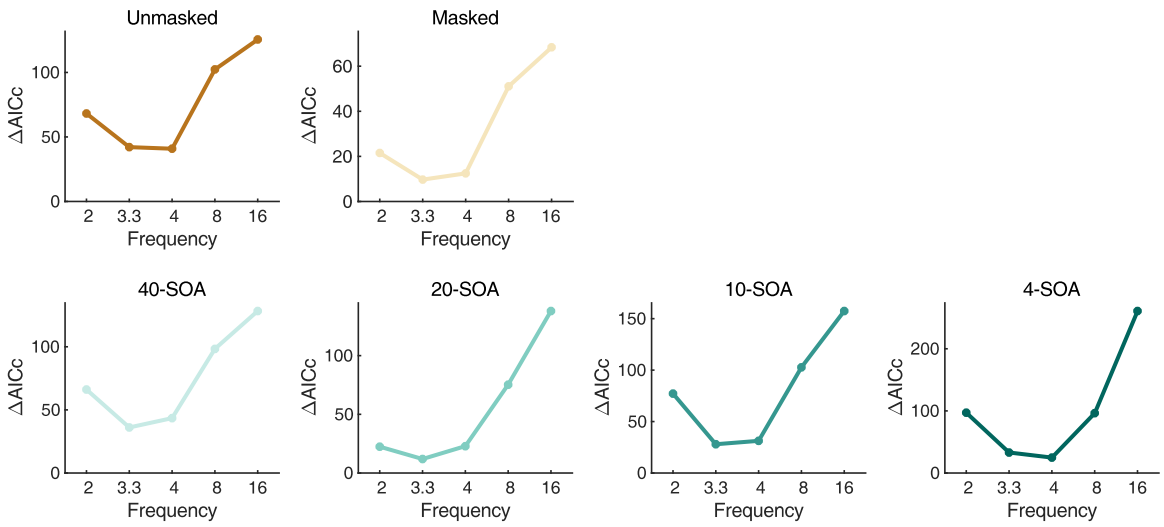

Figure 2-figure supplement 2. Goodness-of-fit of OTEM as a function of the assumed attentional oscillation frequency. For the model fitting results presented in the text and the other plots, the frequency of attentional oscillation was fixed to 3.3 Hz (see Methods). Here we compared the model fitting results that were based on different frequencies including 3.3 Hz. The smaller the AICc, the better the goodness-of-fit. “Unmasked” and “Masked” respectively refer to the unmasked and masked priming experiments of Huang et al. (2015). “40-SOA”, “20-SOA”, “10-SOA”, and “4-SOA” refer to the four temporal context conditions in the new experiment. In all the experiments, the best fit occurred at 3.3 or 4 Hz, suggesting a theta-band attentional oscillation.

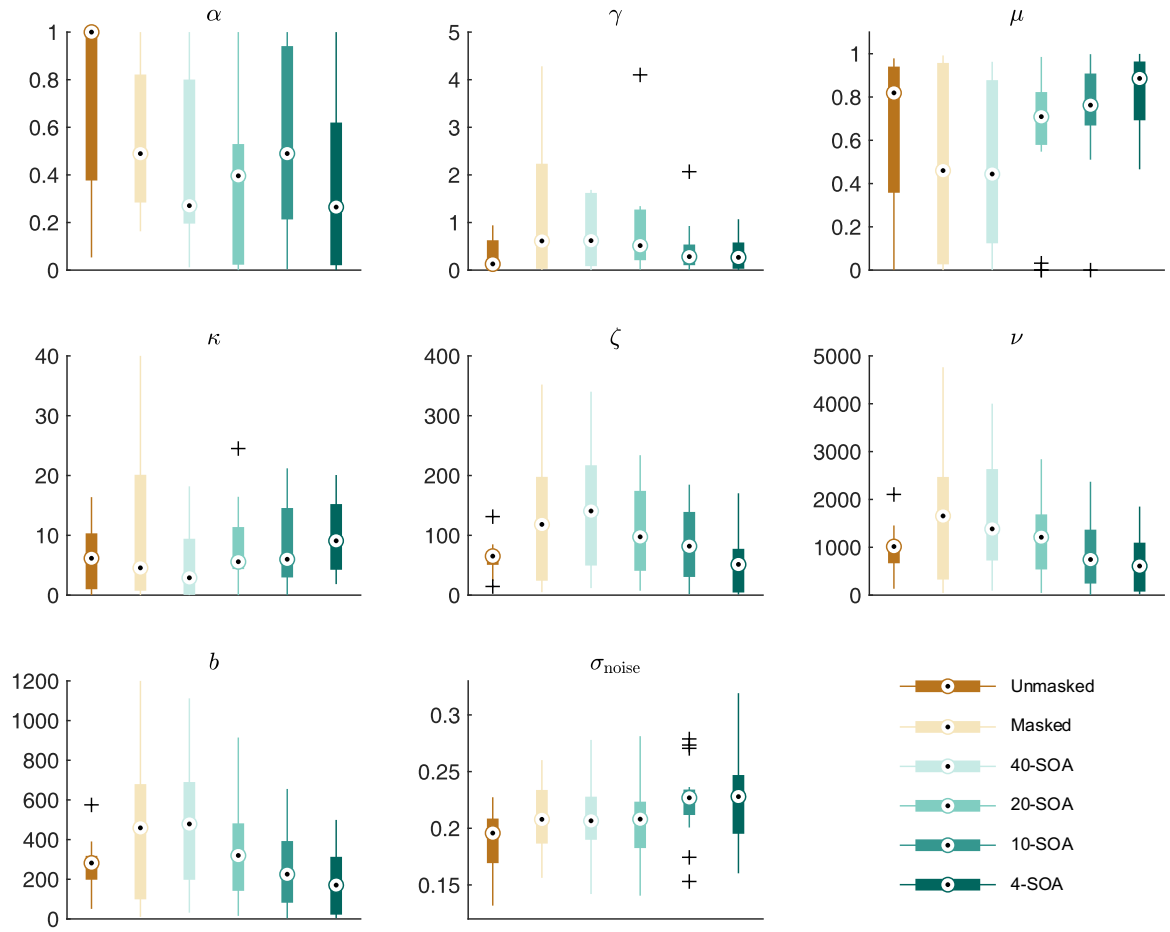

Figure 2-figure supplement 3. Estimated parameters of OTEM. Black dots denote medians. The bottom and top edges of bars respectively indicate the 25th and 75th percentiles. Plus signs denote outliers. “Unmasked” and “Masked” respectively refer to the unmasked and masked priming experiments of Huang et al. (2015). “40-SOA”, “20-SOA”, “10-SOA”, and “4-SOA” refer to the four temporal context conditions in the new experiment.

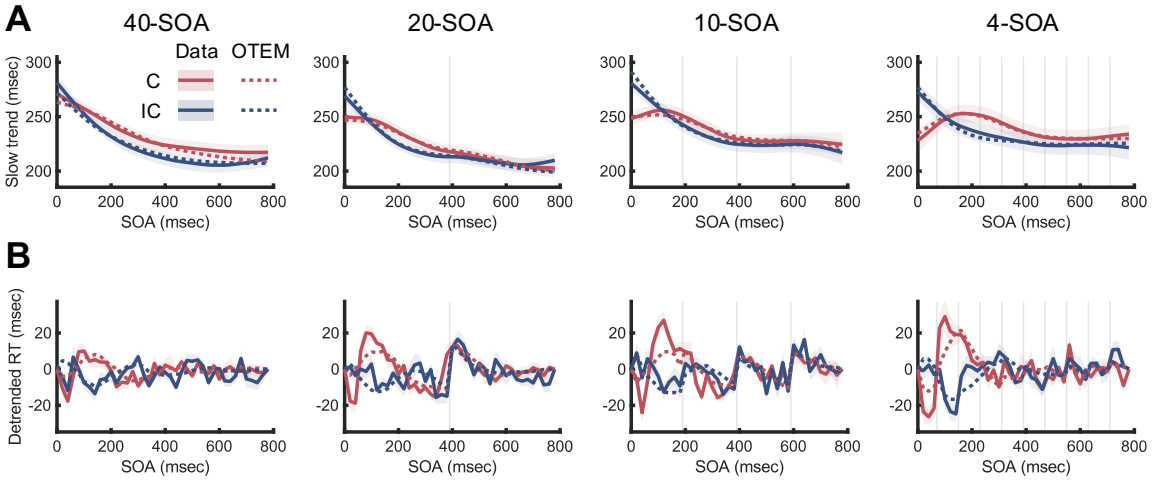

Figure 3-figure supplement 1. **Slow trend and detrended RT for the new experiment: data versus OTEM fits. A**, slow trend of RT as a function of SOA. **B**, detrended RT as a function of SOA. Each column denotes one temporal context condition. Conventions follow **Figure 3**. The OTEM fits agreed well with data in both the slow trend and detrended RT.

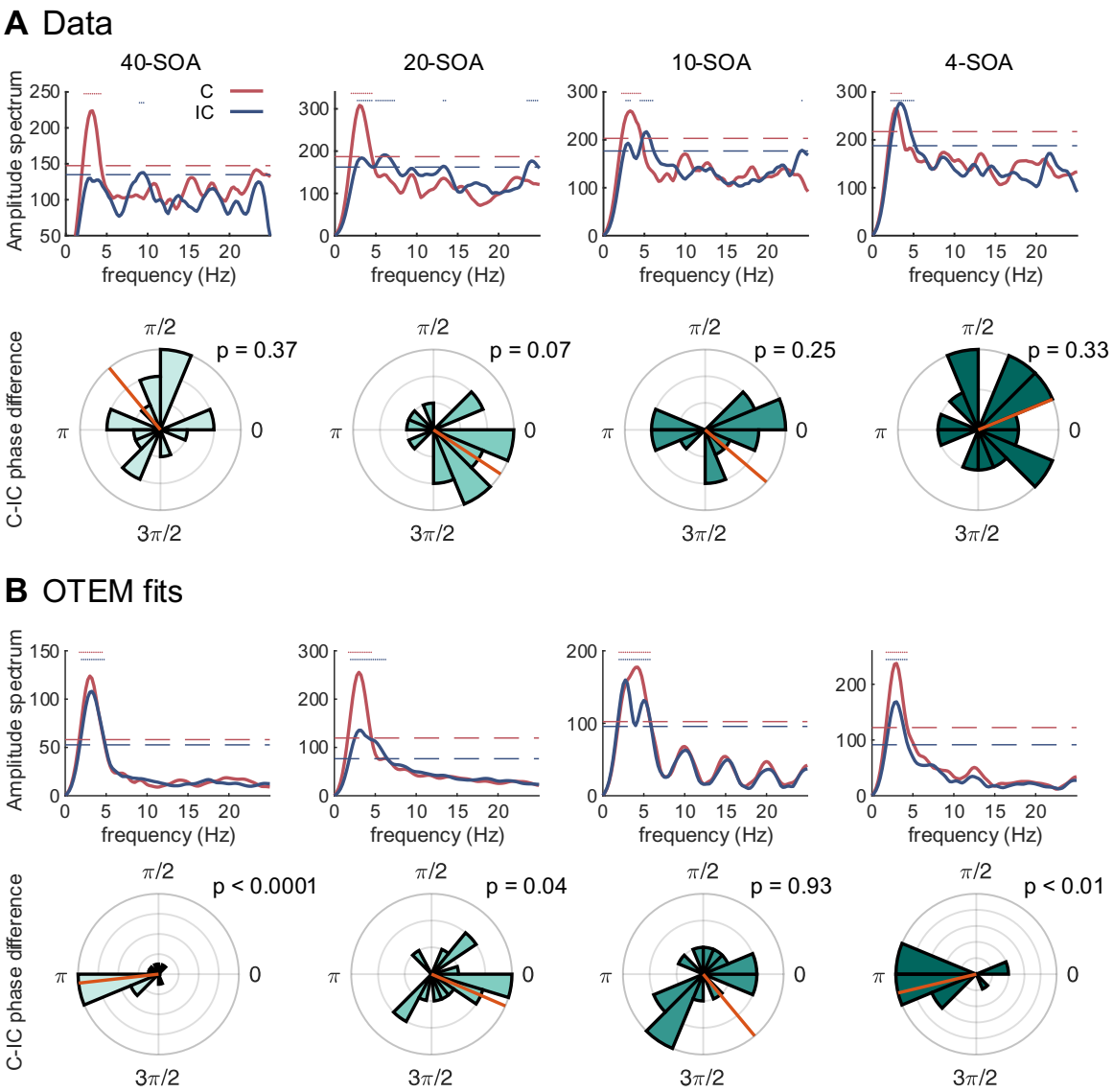

Figure 3-figure supplement 2. **Spectral analysis of the detrended RT for data (A) and OTEM fits (B) in the new experiment.** Each column denotes one temporal context condition. Upper panels: amplitude spectrum. Dash lines denote the 0.05 significance threshold of permutation test (corrected for multiple comparisons). Significant frequency points are marked by dots above the spectrum curves. Significant theta-band oscillations were found in the data for all conditions except for the congruent in the 40-SOA condition. Significant theta-band oscillations were also found in the OTEM fits. Lower panels: phase difference between the congruent and incongruent in theta-band oscillation (3–5 Hz). The phase differences of OTEM fits were close to those of real data in all conditions except for the 4-SOA condition. Conventions follow **Figure 1-figure supplement 1**. See

Methods for the spectral analysis and multiple-comparison correction methods. That the theta peak for the incongruent in the 40-SOA condition failed to reach significance may be a Type II error in statistics, that is, failing to reject the null hypothesis when the alternative hypothesis is true. Even when the statistical power of a single test is as high as 0.9, the probability of committing at least one Type II error out of 12 tests ([congruent, incongruent] $\times$ 6 conditions in the three experiments) is above 70%.

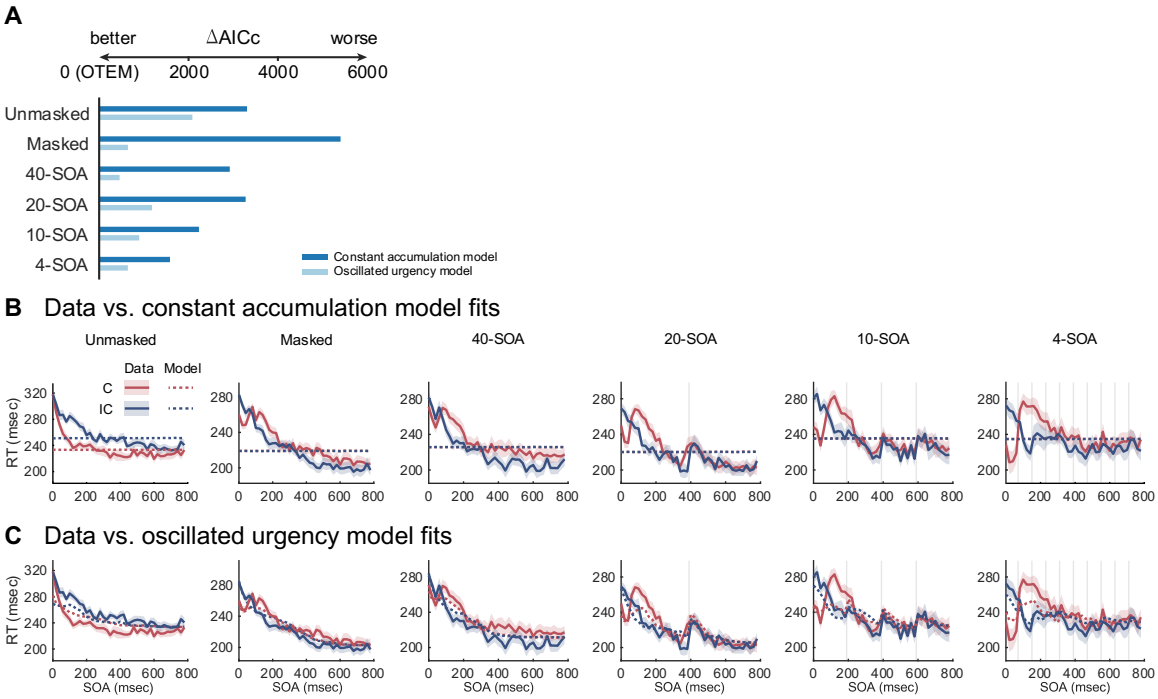

Figure 3-figure supplement 3. OTEM outperforms alternative models. A, The ΔAICc of the oscillated urgency model and constant accumulation model relative to that of OTEM. In all experiments and conditions, both alternative models fit to the RT data considerably worse than OTEM did. **B**, data (solid lines) vs. constant accumulation model fits (dotted lines). **C**, data (solid lines) vs. oscillated urgency model fits (dotted lines). Conventions follow **Figure 3**. “Unmasked” and “Masked” respectively refer to the unmasked and masked priming experiments of Huang et al. (2015). “40-SOA”, “20-SOA”, “10-SOA”, and “4-SOA” refer to the four temporal context conditions in the new experiment.

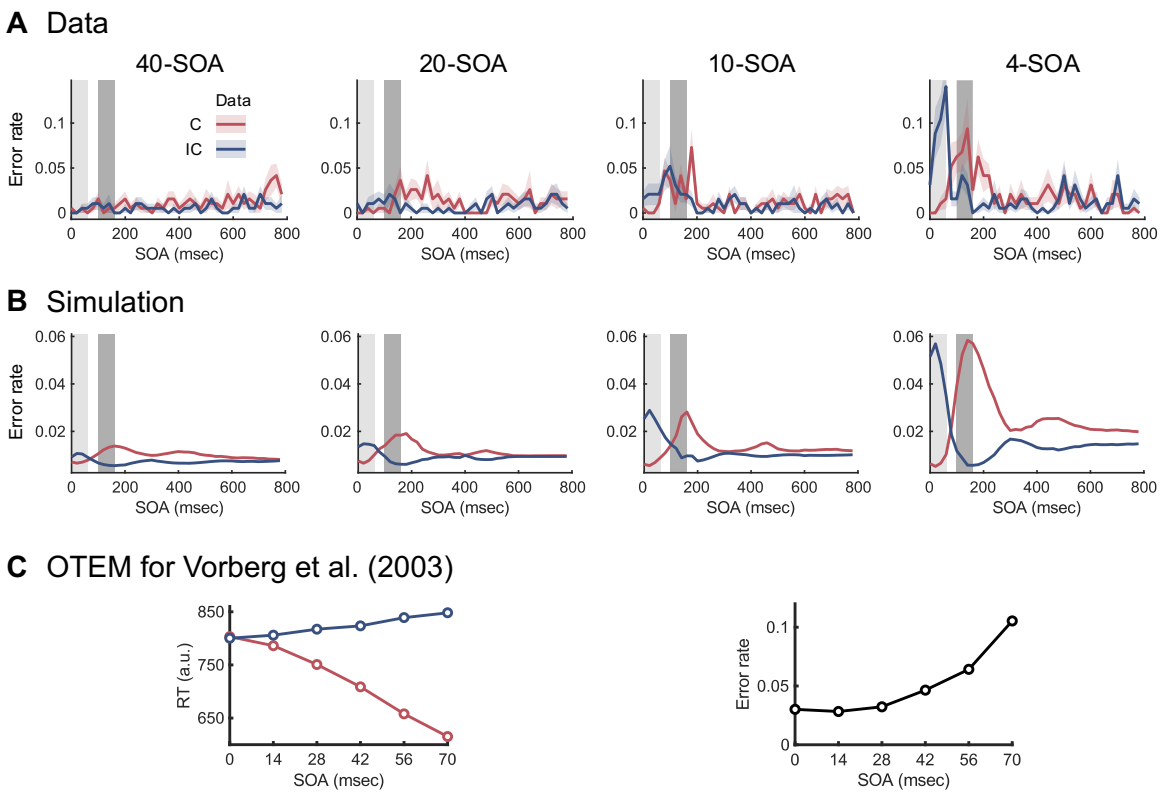

Figure 3-figure supplement 4. Extended OTEM explains error rates and atypical priming effects. A, mean error rate as a function of SOA, separately for the congruent (red) and incongruent (blue). Shadings around the mean error rates denote SEM. Light and dark gray shadings respectively denote the time intervals around the peak of positive and negative priming. Each panel is for one temporal context condition. **B**, mean error rate simulated by the extended OTEM, which reproduced the empirical pattern: positive priming was accompanied by a higher error rate for the incongruent and negative priming by a higher error rate for the congruent. **C**, mean RT and error rate simulated by the extended OTEM for the visual priming task of Vorberg et al. (2003), which captured the atypical patterns of their empirical findings: RTs for the congruent and incongruent respectively decreased and increased with SOA; error rates increased with SOA.